separations

MDPI

Article

Innovating Slow Sand Filtration: Exploring the Regeneration of a Traditional Technology for the 21st Century

Hayley Corbett [1,*], Brian Solan [1], Svetlana Tretsiakova-McNally [1], Pilar Fernandez-Ibañez [2], Bárbara Luíza Souza Freitas [2,3] and Rodney McDermott [1]

[1] Belfast School of Architecture and the Built Environment, Ulster University, Belfast BT15 1AP, UK; b.solan@ulster.ac.uk (B.S.); s.tretsiakova-mcnally@ulster.ac.uk (S.T.-M.); r.mcdermott@ulster.ac.uk (R.M.)
[2] School of Engineering, Ulster University, Belfast BT15 1AP, UK; p.fernandez@ulster.ac.uk (P.F.-I.); barbaralsfreitas@usp.br (B.L.S.F.)
[3] Department of Hydraulics and Sanitation, São Carlos School of Engineering, University of São Paulo, Avenida Trabalhador São-Carlense 400, São Carlos 3566-590, Brazil
* Correspondence: corbett-h1@ulster.ac.uk

Abstract

The intensifying rate of global water stress is motivating the exploration of alternative water sources. This research aims to unlock conventionally unusable wastewater effluent for reuse with the aid of slow sand filtration (SSF). In this study, a traditional SSF reactor was constructed and later modified by replacing a section with sawdust, a sustainable material. The two filter configurations were asynchronously investigated to evaluate their potential capacity for the removal of antibiotics and common surface-water nutrients, i.e., nitrates and phosphates. Each filtration system was operated in a recirculating mode over four weeks to develop the biological component referred to as the "schmutzdecke". Standard water-quality testing indicated that the SSF with an incorporated sawdust layer buffered shock events (e.g., turbidity spikes) while still cultivating a healthy schmutzdecke. Furthermore, the sawdust facilitated greater microbial activity, which is associated with the biodegradation of various contaminants and pathogens. Following filtration of a simulated wastewater effluent containing sulfamethoxazole (SMX) and trimethoprim (TMP) antibiotics (ca. 1 mg·L^{-1}), it was found that the TMP removal exceeded 93% in both configurations. The SMX removal rate was much lower and varied significantly, ranging from 1.2 to 38.6% and from 1.4 to 3.4% for the traditional and modified filters, respectively. These findings suggest that the proposed configuration has the potential to address some emerging contaminants but that refinements are needed to address other contaminants such as SMX.

Keywords: environmental pollutants; slow sand filtration; lignocellulose; emerging contaminants; wastewater treatment

Check for updates

Academic Editors: Nuan Yang and Bing Yang

Received: 28 May 2026
Revised: 4 July 2026
Accepted: 8 July 2026
Published: 10 July 2026

Copyright: © 2026 by the authors. Licensee MDPI, Basel, Switzerland. This article is an open access article distributed under the terms and conditions of the Creative Commons Attribution (CC BY) license.

1. Introduction

Global water stress is progressing as existing water sources are subjected to increasing pressure from growing industrial and domestic usage and deteriorating quality [1]. Ageing infrastructure, emerging contaminants, insufficient legislation, increasing agricultural needs, and accelerating industrial usage all pose unique risks to our most valuable resources [2,3]. As reported in 2024 only 56% of domestic wastewater produced globally is safely treated [4]. While in Europe and Northern America this proportion is as high as 87%, in Latin America and the Caribbean the proportion is only 37%, despite having comparable

human development index scores, with both regions placed in the high human development bracket [5]. A further complication is the challenge to satisfy new treatment standards using the current ageing wastewater infrastructure [6]. The 2024 revision to the Urban Wastewater Directive has introduced the necessity to address specific micropollutants in wastewater. The amendment mandates that large wastewater treatment plants (WTPs) implement quaternary treatment by 2045, and will be assessed using specific indicator compounds (pharmaceuticals and other cosmetic residues) where a minimum of 80% removal is required [7]. This underscores the need for innovative water treatment approaches which are accessible to decentralised communities, while also promoting sustainable, circular economy principles that can be utilised by all.

Current wastewater treatment plants and existing standards are insufficient to adequately remove challenging pollutants from discharges, including contaminants of emerging concern (CECs), such as pharmaceuticals and personal care products (PPCPs), resulting in their widespread persistence in the aqueous environment [8]. Subsequently, as an approach to controlling CECs discharges, a variety of adsorbent materials were proposed and studied, including biochar and activated carbon (AC) [9,10] and their precursor, sawdust [11,12]. Whilst AC boasts excellent adsorption capacities, the full potential of sawdust is yet to be elucidated. Likewise, the production of AC can be cost- and energy-intensive, whereas sawdust features a lower cost and abundant feedstock since it is a waste biomass resource. Furthermore, much of the present literature is focused on batch adsorption experiments, which mainly investigate the sorbent-contaminant kinetics. Other reported studies which utilise fixed-bed filter treatments are predominantly small-scale and low-volume. Recent publications on slow sand filtration include a 2025 study on rainwater purification that examined the roles of the biofilm and water phases in 60 cm-deep columns [13], as well as a separate study demonstrating the utility of SSF for treating dairy wastewater using 45 cm of filtration media [14]. Together, these studies underscore the promise of SSF for rural, decentralised treatment and wastewater reuse. However, further work is needed to move beyond small-scale laboratory systems and to better understand the operational challenges associated with scaling SSF toward engineered prototype applications.

Slow sand filters (SSFs) provide an excellent model for retrofitting with adsorbent materials, as is often seen in AC filters [9,10]. SSFs are occasionally used as modular polishing steps (tertiary treatment) within larger treatment trains after pre-treatment and before further disinfection or other processing [15]. SSF configurations are typically limited in size and scope due to constraints of space, available monetary resources, influent supply, and effluent handling, especially during the ripening of the filter when effluent water quality is substandard for direct discharges. In addition, the operational and biological restrictions with traditional SSFs may limit its maximum potential. Therefore, the current investigation outlines an innovative solution to minimise obstacles in SSF research, focusing on the recirculation of effluent in a closed loop to provide nutrients to the biofilm substrate and for stabilisation of the schmutzdecke. This is the biological layer which enhances water remediation. While recirculation is widely used in municipal SSF ripening [15] to conserve water and limit waste, it remains largely unexplored in the literature for true down-flow SSF designs at pilot or full scale. Investigations of SSF in the literature often focus on single-pass systems, where the effluent runs to waste, even during the filter ripening period. Aside from mere filter ripening, recirculating filters are commonly employed in aquaculture systems for the cultivation and farming of fish [16], and in aquaponics to enable nitrification of water in soil-less cultivation of different plants [17]. Closed systems are also utilised in cooling systems (e.g., data centre cooling) to control the biological quality of the water and to limit the corrosion of equipment. While water in these systems is often chemically treated, filtration can also be applied [18] as a sustainable, cost-effective alternative.

Few studies have demonstrated recirculating biofilters [19,20], but these do not translate to operational conditions, bed depths, or hydraulic loads relevant to public or industrial slow sand filters. In the current work, a recirculating system is examined for its capability to cultivate a healthy schmutzdecke with limited nutrients and microorganisms. The present study aims to address this gap by evaluating a recirculating down-flow SSF at pilot-scale, considering how operational configuration affects contaminant removal, with a focus on a novel sustainable adsorbent with lignocellulosic structure (i.e., treated sawdust), to enhance performance potential.

2. Materials and Methods

2.1. Materials

Chemicals were used as received directly in experiments without further purification steps. The HPLC-grade antibiotics (≥98%), trimethoprim ($C_{14}H_{18}N_4O_3$) and sulfamethoxazole ($C_{10}H_{11}N_3O_3S$), both in powdered forms, were purchased from Merck (Sigma-Aldrich, St. Louis, MO, USA). Type I water (PURELAB Option Q DV, Elga LabWater, Lane End, UK) was used to prepare solutions of antibiotics unless otherwise stated. Stock solutions were stored in amber glassware, protected from exposure to light, and at 4 °C. All the sand used in the experiments was sourced from a working WTP (Ballyshannon WTP, Co., Donegal, Ireland). The sand was existing stock material and had no prior exposure to water treatment processes. The sawdust material was acquired locally from a sawmill and air-dried before further processing as outlined in the Supporting Information (SI, Text S1).

2.2. Filter Design and Construction

In this study, the SSF test reactor was designed using the optimal parameters elucidated from a review of the literature published by the authors [6]. These are summarised in Table 1. While the review did not identify a single optimal filtration rate for contaminant removal or subsequent daily treated water volumes, the Centre of Affordable Water and Sanitation Technology (CAWST) recommends a maximum of 0.4 $m{\cdot}h^{-1}$ for intermittently operated bio-sand filters [21], whereas the Irish Environmental Protection Agency (EPA) recommends ≤0.35 $m{\cdot}h^{-1}$ for continuously operated SSF [15]. Higher filtration rates increase treated water volume, whereas lower rates can generally promote enhanced effluent quality [22], so the optimal filtration rate depends on the contextual demand for water and target effluent standards. For this study, we selected 0.40 $m{\cdot}h^{-1}$ to allow for some expected slowing as the schmutzdecke develops, and this rate was set by controlling the effluent outlet flow rate appropriately.

The slow sand filter (Figures 1 and 2) was manufactured and operated indoors in a laboratory outfitted for hydraulics research for the Belfast School of Architecture and the Built Environment (Ulster University). The filter column comprised a 160 mm internal diameter polyvinyl chloride (PVC) soil pipe. Each of the two reservoirs (upper and lower) was a rectangular 20-gallon (90.9 L) water storage tank. Piping connections were made of white polybutylene and had a 22 mm internal diameter. The water flow was controlled by 22 mm level brass ball valves, labelled as a, b, and c (Figure 1). Materials were sourced from Beggs and Partners (Belfast, Northern Ireland). A water transfer pump was controlled by a float switch in the upper reservoir, enabling refilling of the tank with the filter's effluent when the level reaches a pre-programmed level. This recirculation ensured a constant supply of feeder water to the filter. Extensive detail of manufacture and operation is given in the Supporting Information (Text S1).

Table 1. Recommended characteristics of a typical slow sand filter.

	Parameter or Feature	Recommendation of Review [6]	Other Notes
Filter characteristics	Depth	At least 0.6 m	Depths of larger-scale, down-flow SSFs in the review ranged from 0.40 to 1.0 m; however, greater depths increase removal capabilities. Specifically, 0.6 m is required for virus removal [6].
	Particle effective size (D_{10})	Between 0.15 and 0.40 mm	Smaller particle sizes increase the range of contaminants to be removed, but slow the rate of filtration.
	Particle uniformity co-efficient (C_U)	<2 (highly uniform)	Uniformity of filtration beds influences the retention and thus the contact time between schmutzdecke and contaminants.
	Material chemistry	High silica (typically > 95% SiO_2) content or quartz sand	Important for biofilm adhesion and particle size, shape, and friability.
	Alternative filter materials	High-carbon materials such as anthracite and charcoal enhanced contaminant removal	Production of activated carbon is energy-intensive and requires regeneration/reactivation to be recycled; this impacts the carbon assessment of the treatment process.
		Lignocellulose derived from sawdust waste has potential in the removal of a range of CECs	Tested only on bench-scale with batch and fixed-bed experiments.
	Dimensions	Taking into account constant hydraulic head depths, otherwise at the discretion of its application: • Household vs. community serving filtration • Continuous vs. intermittently operated • Water demand vs. raw untreated water supply	Intermittently run filters are typically more compact and have a smaller hydraulic head to accommodate oxygen incorporation for biofilm survival during idle periods, whereas continually operated filters boast greater volumes of treated water.
	Impact of contaminants on schmutzdecke	Antibiotics may have some influence on the success of biofilm growth and contained microbial communities	More research is needed to fully assess the long-term effects, e.g., antibiotic resistance.

The drainage support was first added to the filter column in the form of a mesh bag containing 3.5 kg of crushed stone (coarse gravel 1–3 cm in diameter). This section filled the bottom of the filter up to 130 mm from the base, preventing the migration of sand material out of the filter through the effluent outlet. New (unused) sand was subsequently added to the filter column in 100 mm increments and tamped down to ensure homogeneous compaction. In terms of particle size distributions (determined by the sieving method used in the current UK standard [23]), the sand had a D_{10} of 0.329 mm, a D_{60} of 0.596 mm, and a subsequent C_U of 1.814. The column was connected to the system, filled with tap water, and left to recirculate for a minimum of 24 h to allow de-gassing of chlorine, if any, from the recirculation water. Total and free chlorine levels were monitored (Chlorine + eXact® EZ photometer, Industrial Test Systems Europe LTD, Salisbury, UK) before the spike of microorganisms to prevent adverse effects on the development of the biofilm.

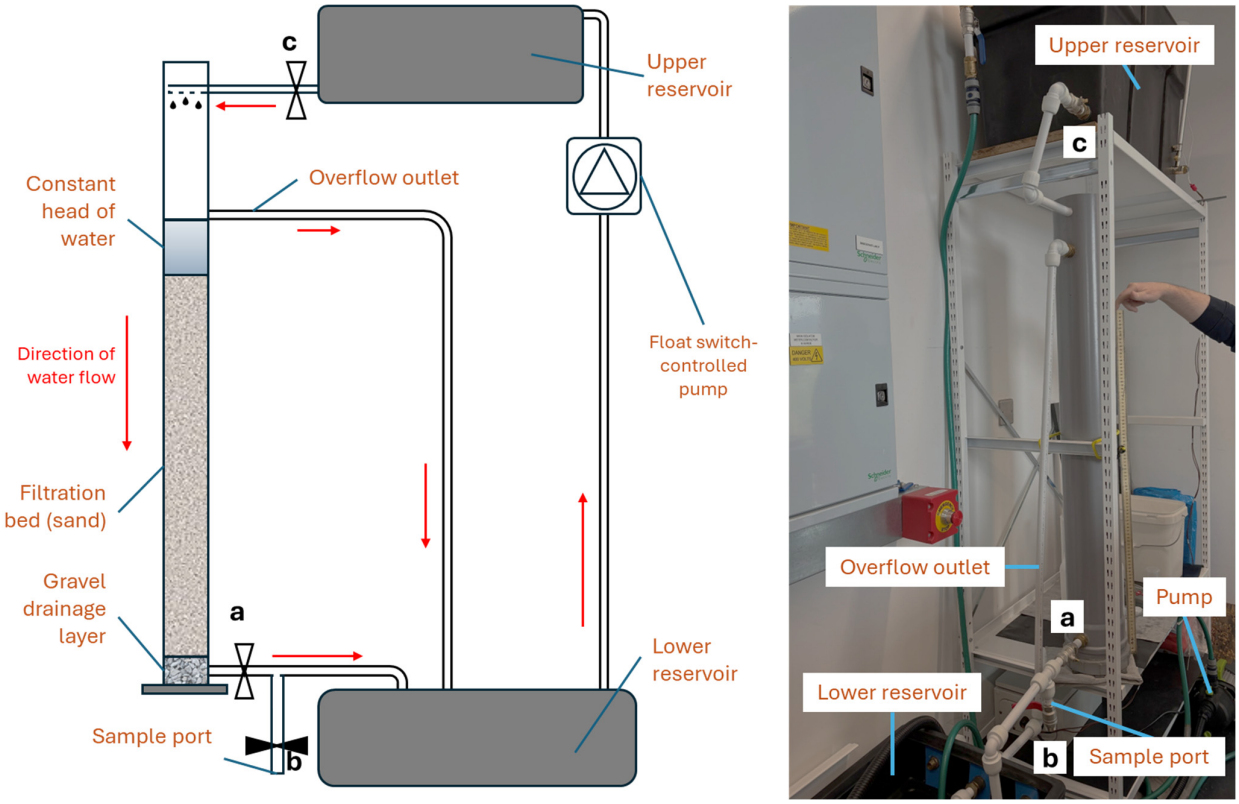


Figure 1. A schematic diagram of the slow sand filter and its recirculating arrangement (**left**), and a digital photograph showing the slow sand filter set-up in operation with a 1 m ruler for scale (**right**) (a: outlet valve which controls filtration rate; b: filtrate sample port; c: upper reservoir valve which controls overflow flow rate; red arrows indicate direction of water flow).

2.3. Operation and Monitoring of the Recirculating Slow Sand Filter

Environmental samples of water obtained from a local urban drainage pond (The Waterworks, Belfast, Northern Ireland; 54°37′28.8″ N 5°56′37.1″ W) were introduced to the filtration system to provide the filter with a community of microorganisms. The samples were collected the same day they were introduced to the system and stored at 4 °C until required. A weekly nutrient feeding regime was applied to support the microbial community and biofilm growth. The nutrient feeding solution was introduced via the upper reservoir, loading the system with carbon, nitrogen, and phosphorus to a target of 5 mg·L^{-1} C, 1.5 mg·L^{-1} N, and 0.5 mg·L^{-1} P (C:N:P = 10:3:1). The ratio of nutrients was chosen based on works by Desmond et al. [24], which corresponded to balanced growth of biofilm structures and stable hydraulic resistance (as opposed to P- or N-limited conditions).

The samples obtained from the overflow pipe served as pre-filtration untreated water for comparison, and those obtained from the sample port served as post-filtration effluent (valve b, see Figure 1). Analysis of water quality was carried out at least three times a week, from the beginning of each experiment until the final day of operation, for the water quality parameters outlined in Section 2.7.

Operational parameters were also monitored as part of the system's quality control. The water level in the lower reservoir was indicative of the water level in the entire system; thus, this was controlled by topping up with dechlorinated water to minimise impact on the water quality parameters by evaporation and removal of sample volumes. Flow rates were measured and recorded at least three times per week, at both the filtrate sample port and the overflow pipe. The valves were set at the beginning of the experiment; thus, the filtration rate was in line with the recommendations (~0.35 m·h^{-1}) [6], and the rate of overflow was sufficient for sampling and to facilitate a constant head depth of 100 mm. The upper

reservoir was agitated at least once a week to prevent the build-up of suspended matter in the narrow opening of the ball valve. The filter was operated in a temperature-controlled laboratory; however, heat fluctuations occurred due to the building's heating, ventilation and air conditioning (HVAC) operation and solar gain through windows. As variations in ambient temperature can influence biofilm development [15,25], the room temperature was recorded from a wall-mounted thermostat at each sampling event. Temperature control within the building was managed by the institution's Estates Department, which determined heating schedules.

The investigation was performed in two parts: the sand-only control (traditional slow sand filter; TSSF) and subsequently, the sawdust hybrid slow sand filter (SDSSF). The control experiment was conducted to establish a baseline for a traditional slow sand filter. Each experiment was performed over 4 weeks, and on the final day, the system was disconnected and challenged with a simulated wastewater effluent (SWWE) containing antibiotics (described below in Section 2.4). Following the control experiment, a new experimental filter was prepared to investigate the performance of the sawdust layer in the slow sand filter water treatment process. The filter was assembled using the same cleaned pipework but with new sand, obtained from the source with a similar particle size distribution. This filter was constructed similarly to the control, except that a layer of sawdust replaced the portion of sand between 20 and 25 cm from the surface of the filter bed. This depth was chosen since the upper 20 cm of the bed contained over 75% of the total microbial activity in the filter, as concluded from the control experiment (see Section 3.4.1). This experimental filter was operated and monitored for just under 4 weeks (27 days), at which point it was also subjected to SWWE.

2.4. Challenging the Filters to SWWE with 2 mg·L^{-1} of Antibiotics

Following the recirculation period of 4 weeks, the system was disconnected and reconfigured for a once-through challenge phase. This consisted of spiking the upper reservoir (approx. 67 L) with a highly concentrated stock of contaminants so that the final influent dilution was close to the composition of SWWE previously reported [26] (Table 2). The SWWE also included a final target concentration of 1 mg·L^{-1} each of trimethoprim (TMP) and sulfamethoxazole (SMX), two antibiotics often prescribed together, which have notable occurrences in various soil and water matrices [27]. This influent was introduced to the system via the upper reservoir. While valves were adjusted to maintain the flow rates as before, these were also monitored at each sampling event. The samples were obtained after 1 h of operation to ensure recirculation water had been completely expelled.

Table 2. Composition of the SWWE and target final concentrations of each contaminant.

Compound	Concentration (mg·L^{-1})
$NaHCO_3$	98.2
$CaSO_4 \cdot 2H_2O$	60.5
$MgSO_4$	581.1
NaCl	4.1
KCl	1.6
Peptone	3.5
Humic acid	4.2
Lignosulfonic acid sodium salt	1.4
Sodium dodecyl sulphate	3.0
Gum Arabic from acacia tree	4.6
$(NH_4)_2SO_4$	25.0
H_2KO_4P	7.7
Trimethoprim	1.0
Sulfamethoxazole	1.0

The removal of each antibiotic was calculated after quantifying the respective concentrations in the influent (overflow sample) and effluent (filtrate sample) using Equation (1).

$$\% \text{ Removal} = \frac{[\text{Influent}] - [\text{Effluent}]}{[\text{Influent}]} \times 100\% \quad (1)$$

where concentrations [Influent] and [Effluent] were measured using an HPLC (Section 2.8) in $mg \cdot L^{-1}$.

2.5. Fluorescein Diacetate Assay

Fluorescein Diacetate Assay (FDA) was implemented to investigate the microbial activity in the filter using enzyme activity as a surrogate indicator. The reaction of the assay is as follows: FDA, which is colourless in solution, is hydrolysed by enzymes to liberate a yellow-green aqueous solution of fluorescein. The density of the microbial community present in a sample is directly proportional to the amount of fluorescein released in the FDA hydrolysis [28].

At the end of each experiment, the filter column was left to drain at a constant rate to prevent hydraulic disturbance of the biomass. Following this, the column was inverted, and the filtration material was removed in a controlled manner. The samples were immediately obtained at pre-determined sections of the core and stored in sterile sample containers at 4 °C until analysis (less than 24 h). The sampling sections were 0–5 cm, 5–10 cm, 10–20 cm, 20–40 cm, 40–65 cm, and 65–90 cm. An additional sample was obtained from the filter containing sawdust between 20 and 25 cm to characterise microbial activity in solely this material. Additional samples of sand were also assayed to confirm baseline FDA concentrations of unused and sterile sand (unused sand heated in an oven at 121 °C for 24 h).

For the assay, a protocol adapted from [28,29] was implemented. Circa 2 g of the sample was weighed into a 50 mL Falcon tube with 15 mL potassium phosphate buffer (pH 7.6). The reaction was commenced upon the addition of 0.2 mL of 1000 $\mu g \cdot mL^{-1}$ FDA solution to all the samples (performed in triplicate) except reagent blanks (which were prepared for each section 0–5 cm, 5–10 cm, etc.). Following shaking by hand, the closed tubes were incubated at 30 °C for 20 min. Under local exhaust ventilation, 15 mL of a reaction terminator reagent (chloroform/methanol ratio 2:1) was added immediately to each tube following incubation, and the closed tubes were shaken by hand again. All the tubes were centrifuged at 2000 rpm for 3 min. The supernatant of each was carefully decanted using 5 mL pipettes and analysed using a spectrophotometer (Jenway 6305 Spectrophotometer, Bibby Scientific Ltd, Staffordshire, UK) at 490 nm. A calibration curve was prepared using standards of appropriate dilution of fluorescein sodium salt (Vital Minerals, Lancashire, UK), using potassium phosphate buffer to dilute and as a blank. From this, the concentration of fluorescein was calculated, and the resulting enzyme activity was expressed in mass of fluorescein per mass of dried filtration media ($\mu g \cdot g^{-1}$).

2.6. Microscopy

The remnants of the samples obtained for the FDA (see above) were retained to capture images of the microorganisms present in the various depths. Drops of the supernatant were removed just above the surface of the sample to withdraw as much of the biological matter as possible, and each drop was visualised under brightfield microscopy (Motic BA310E, Motic Incorporation Ltd., Kowloon, Hong Kong) under ×40 and ×100 magnification objectives with a ×10 magnification binocular lens (total magnification ×400 and ×1000, respectively). The environmental water samples were also analysed following centrifugation at 1000 rpm for 10 min, removing the pellet and viewing under a microscope

as before. Images were processed using ImageJ (v1.54g) [30]. The main microorganisms were identified for each depth sample, and the different specimens were identified down to the lowest taxonomic level possible. The works of [31,32] were utilised in identifying microorganisms by comparison.

2.7. Water Sample Analysis

The samples obtained from the filter, as well as the environmental freshwater samples, were subjected to a panel of standard water testing parameters. The samples were tested in triplicate. Turbidity was measured using a Hach 2100Q turbidimeter (Hach Lange GmbH, Düsseldorf, Germany), pH using a Mettler Toledo S20 SevenEasy™ pH meter (Mettler-Toledo, Colombus, OH, USA), and dissolved oxygen (DO) using a Hach HQ30D DO meter (Hach Lange GmbH, Düsseldorf, Germany). Concentrations of nitrates [NO_3^-] and reactive phosphorus (ortho-phosphates, [PO_4^{3-}]) were determined using spectrophotometry (Hach DR/2500 spectrophotometer, Hach Lange GmbH, Düsseldorf, Germany) utilising the cadmium reduction method and ascorbic acid method, respectively. Electrical conductivity (EC) was measured using a Jenway 4200 probe (Jenway, Stone, UK). Total dissolved solids (TDS) can be calculated using the EC, as per Equation (2):

$$TDS = k \cdot EC \quad (2)$$

where TDS is measured in $mg \cdot L^{-1}$, EC is measured in $\mu S \cdot cm^{-1}$, and k is the conversion factor or the ratio, TDS:EC. This ratio varies depending on the type of water and the specific ions dissolved in the sample, typically ranging from 0.5 for distilled water to 0.75 for seawater and brine waters [33]. In this case, the composition of ions was unknown, and the conversion factor of 0.6 was utilised.

Dissolved organic matter (DOM), also referred to as UV254, was roughly estimated using UV-Visible spectrometry (PerkinElmer UV/Vis Lambda 365, PerkinElmer, Inc., Waltham, MA, USA) at wavelength 254 nm following filtering with 0.45 µm cartridges. Enumeration of total culturable bacteria was performed at least once a week by heterotrophic plate counts of both the overflow and filtrate samples (incubated overnight at 35 ± 2 °C on tryptone soya agar; TSA). The bacterial counts in these samples represented the planktonic bacteria (free-floating) recirculating in the filter, separate from the bacteria present in the colonised filter material. The bacteria present in the filter material were immobilised in the schmutzdecke matrix of extracellular polymeric substances (EPSs). Analytical approaches were in accordance with standard protocols [34].

2.8. High-Performance Liquid Chromatography

Quantification of antibiotic concentrations was achieved for the pre- and post-filtration samples using high-performance liquid chromatography (HPLC) using an Agilent Technologies Series 1260 Infinity II system with a UV diode array detector (Agilent Technologies, Waldbronn, Germany). The system was fitted with a Poroshell 120 EC-C18 analytical column with dimensions 4.6 × 100 mm (Agilent Technologies, Waldbronn, Germany). A previously described protocol [26,35] was employed with minor modifications. Briefly, 100 µL of the sample was injected, and a gradient method was employed with a 1 $mL \cdot min^{-1}$ flow rate: 95:5 (v/v) 25 mM formic acid to 98% acetonitrile (2% ultrapure water) continuing to 20:80 (v/v) over 13 min, then from 20:80 (v/v) to 0:100 (v/v) until 14 min. An equilibration post-run of 3 min was applied, and the detection wavelengths for TMP and SMX were 267 and 273 nm, respectively. Calibration curves were prepared using a standard of 1 $mg \cdot L^{-1}$ (1000 $\mu g \cdot L^{-1}$) of each antibiotic in SWWE, which was suitably diluted using the HPLC system's automated dilution function. The limits of detection for TMP and SMX were 13.6 and 10.2 $\mu g \cdot L^{-1}$, respectively.

2.9. Statistical Analysis

Significance tests were conducted using Microsoft Excel®'s (version 2606; Microsoft Corporation, Redmond, WA, USA) *t*-test function for multiple comparisons, where *p*-values of <0.05 were considered significant. Specific tests (homoscedastic, heteroscedastic, one-tailed, two-tailed, and paired) are detailed in the text. Where provided, averages are given as plus or minus one standard deviation, SD, of the mean, M (M ± SD). Error bars presented in graphical figures represent one standard deviation of the mean value.

Spearman's rank correlation co-efficients were used to examine relationships between water-quality parameters of the overflow and filtrate over the duration of the recirculation period for each of the SSFs. The co-efficient, rho (ρ), was calculated from ranked data, with ties assigned average ranks where necessary. Statistical significance was assessed using two-tailed *p*-values derived from the corresponding *t*-statistic with $n - 2$ degrees of freedom (where n was the number of paired observations). This data is available in the Supplementary Information.

3. Results

Each column consisted of identical apparatus and was subjected to the same protocols with regard to feeding of the schmutzdecke. The average filtration rate measured at the outlet of the filter was the same for the TSSF (0.37 ± 0.05 m·h^{-1}, n = 20) and SDSSF (0.39 ± 0.02 m·h^{-1}, n = 15), respectively (p = 0.21, one-tailed homoscedastic *t*-test). The filtration sand used in each case was of the same batch and thus had an analogous particle size distribution, as confirmed through particle size analysis. Due to the sum of these facts, the results presented in this section were the outcomes of two variables: the replacement of a section of sand with sawdust between 200 and 250 mm below the surface, and the contents of the environmentally derived freshwater samples used to seed the filters with microorganisms.

3.1. Environmental Freshwater Characteristics

The environmental freshwater source was analysed at three different time points: July 2025, September 2025, November 2025 (Table 3) for the water quality parameters outlined in Section 2.3. The samples obtained in September and November 2025 were used to seed the sand-only control (TSSF) and the sawdust hybrid filter (SDSSF), respectively, and physicochemical and biological characteristics of each are spotlighted in Table 3. The characteristics of a sample obtained in July 2025 are included to show seasonal changes, which may be paralleled in the microbial diversity in different niches [36]; however, this is beyond the scope of the current work but was deemed an important point to mention.

Table 3. Environmental freshwater sample quality characteristics.

Parameter	July 2025 (Mean ± SD)	September 2025 (Mean ± SD)	November 2025 (Mean ± SD)
Total bacteria per mL (log)	-	2.65 ± 1.69	2.94 ± 2.03
Turbidity (NTU)	3.32 ± 0.71	3.43 ± 0.19	9.01 ± 2.66
pH	8.16 ± 0.18	8.14 ± 0.03	7.93 ± 0.09 *
DO (mg·L^{-1})	9.49 ± 0.10	9.53 ± 0.14	9.39 ± 0.14
EC (mS·cm^{-1})	0.881 ± 0.000	0.788 ± 0.006	0.671± 0.003 *
TDS (mg·L^{-1})	530.00 ± 2.65	472.80 ± 3.65	402.3 ± 2.08 *
Nitrates (mg·L^{-1})	1.25 ± 0.05	0.47 ± 0.06	0.30 ± 0.20
Phosphates (mg·L^{-1})	0.19 ± 0.01	0.76 ± 0.23	2.53 ± 1.15
DOM (at 254 nm)	0.0680 ± 0.0040	0.1694 ± 0.0023	0.1566 ± 0.0023 *

* indicates that the September vs. November difference is statistically significant ($p < 0.05$, two-tailed heteroscedastic *t*-test).

3.2. Monitoring of Slow Sand Filters

All the comprehensive monitoring results can be found in the Supporting Information document (Figures S1–S4), including the correlation co-efficient (*r*) values for parameters from both the traditional and sawdust-incorporated filter (Tables S1–S6).

Operation of the traditional recirculating SSF occurred between September 2025 and October 2025, totalling 33 days of recirculation. Nutrient supplements were fed to the filter weekly on days 7, 14, 20, and 28 to support schmutzdecke development. Its water levels were checked and topped up with de-chlorinated water as normal.

The sawdust-incorporated recirculating SSF was operated between November 2025 and December 2025. This filter was operated for 27 days, and nutrients were supplemented on days 8, 15, and 22. On day 17 of the experiment, the water transfer pump failed for a short period due to a power outage, and subsequently the water in the upper reservoir was completely drained before the pump could be reset. On the morning of day 18, when the pump failure was discovered, it was noted that the water level above the surface of the sand had dropped just below 10 cm in height. Upon restarting the pump to replenish the upper reservoir and resume recirculation, the rapid refilling briefly increased the flow velocity, which likely caused resuspension of particles which had settled over time and affected parameters sensitive to dissolved oxygen. A set of the summary results is shown in Figures 2–5 herein.

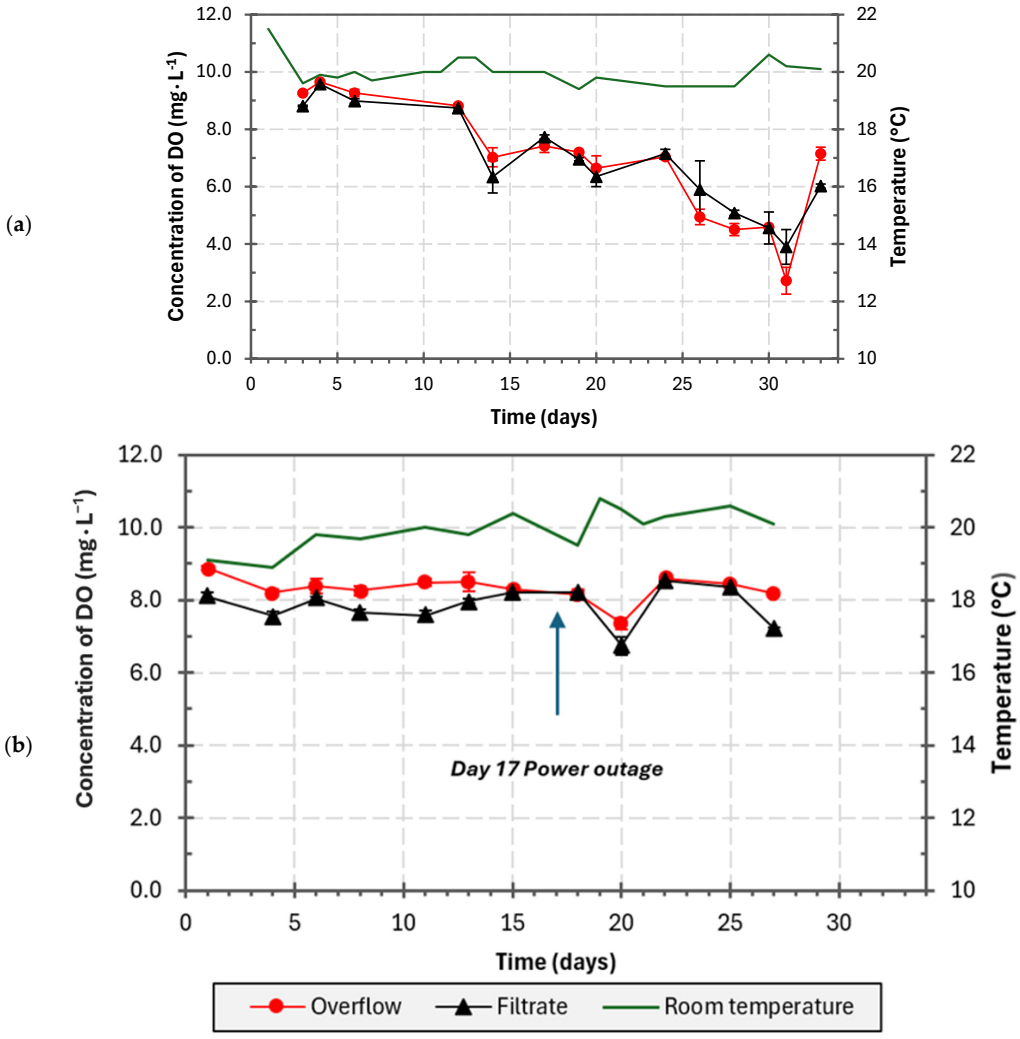
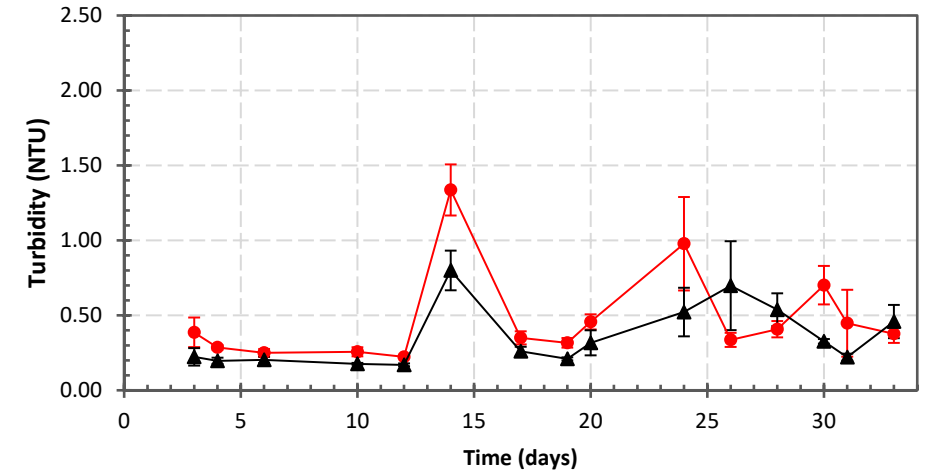


Figure 2. Concentration of dissolved oxygen in overflow and filtrate, and room temperature for the (**a**) TSSF and (**b**) SDSSF. The blue arrow represents the pump failure event outlined in the opening of Section 3.2 (SDSSF only).

(**a**)



(**b**)

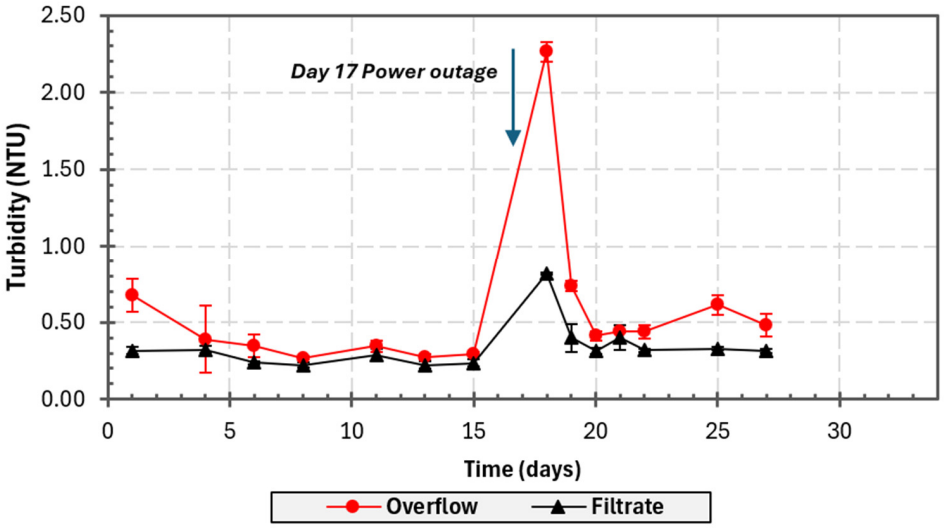


Figure 3. Turbidity values for overflow and filtrate for the (**a**) TSSF and (**b**) SDSSF. The blue arrow represents the pump failure event outlined in the opening of Section 3.2 (SDSSF only).

(**a**)

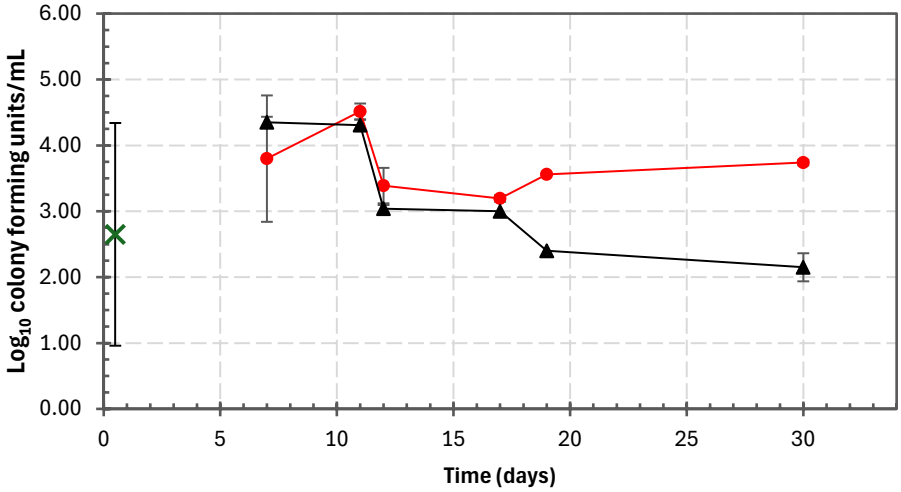


Figure 4. *Cont.*

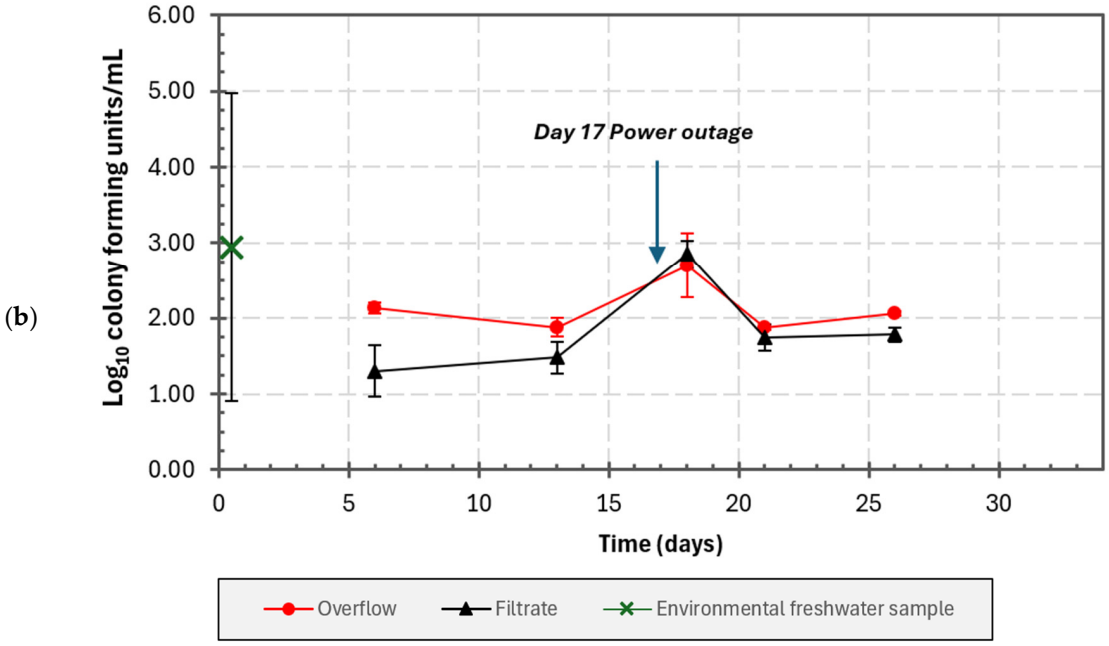


Figure 4. Concentration of bacteria in the overflow and filtrate (heterotrophic plate counts, TSA agar, overnight incubation at 35 ± 2 °C) for the (**a**) TSSF and (**b**) SDSSF. The blue arrow represents the pump failure event outlined in the opening of Section 3.2 (SDSSF only).

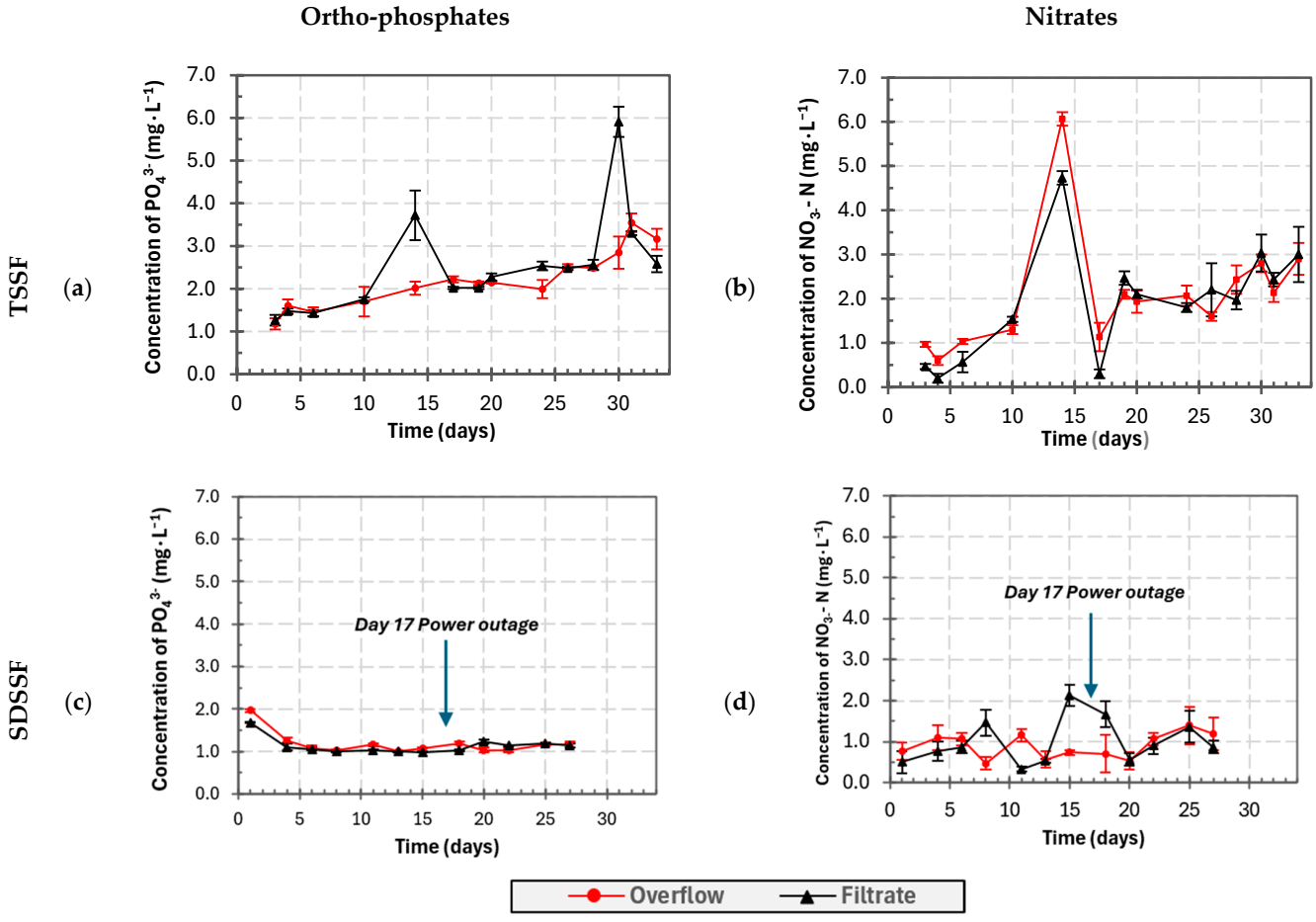


Figure 5. Concentration of nutrients in the overflow and filtrate of each filter: (**a**) Concentration of ortho-phosphate (PO_4^{3-}) in the TSSF; (**b**) concentration of nitrate (NO_3^-) in the TSSF; (**c**) concentration of ortho-phosphate (PO_4^{3-}) in the SDSSF; (**d**) concentration of nitrate (NO_3^-) in the SDSSF. The blue arrows represent the pump failure event outlined in the opening of Section 3.2 (SDSSF only).

3.3. Challenging the Filters to SWWE and Antibiotics

All the comprehensive challenge results can be found in the Supporting Information (Figure S5). The removal of two antibiotics used in this work is outlined in Table 4 and depicted in Figure 6.

Table 4. Percentage removal of two antibiotics using a TSSF and an SDSSF.

Antibiotic	TSSF Mean % Removal ± SD (*p*-Value)	SDSSF Mean % Removal ± SD (*p*-Value)
Trimethoprim (TMP)	93.4 ± 8.8 $^{\Delta}$ (0.005)	98.1 ± 0.6 $^{\Delta}$ (0.00001)
Sulfamethoxazole (SMX)	14.5 ± 20.9 (0.352)	2.3 ± 1.0 (0.060)

$^{\Delta}$ Two or more replicates were quantified below the limit of detection for TMP (13.6 μg·L^{-1}), and thus complete removal can essentially be assumed in these instances.

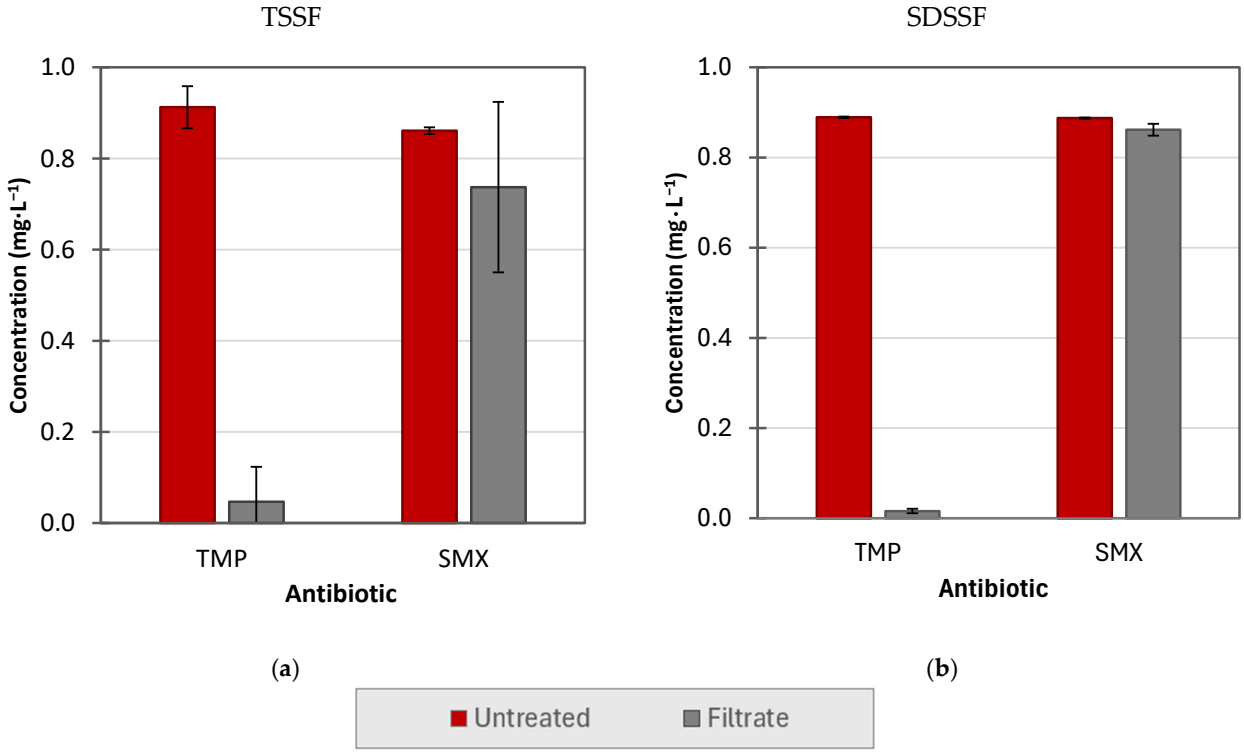


Figure 6. Graphical representation of antibiotic removal in the (**a**) TSSF and (**b**) SDSSF.

3.4. Strata of the Filter Column

The FDA and microscopic visualisation of the filter material enabled comparative examination of the schmutzdecke development zone between the traditional and SDSSF, as well as between sub-sections of the depths themselves. While the microscopy presented straightforward microorganism classifications as an assessment of diversity, the FDA analysis provided quantification of enzyme activity as a surrogate for microbial activity measurement.

3.4.1. Microbial Activity—FDA

During preparation of the samples for the FDA, a greater volumetric portion of the sawdust was required to obtain the ~2 g target mass compared to sand, reflecting the lower density of the lignocellulosic material. Although enzyme activity was initially normalised to dry mass (μg·g^{-1}) as per the protocol, differences in porosity and liquid retention capacity between the materials may have influenced the apparent activity values. In particular, the higher liquid-holding capacity of sawdust could result in greater retention of enzymes.

To account for this, an additional normalisation step was introduced, whereby activity was expressed relative to the mass of liquid lost during drying (evaporation-normalised, assuming liquid has a density of 1 g·mL^{-1}). The results are, therefore, presented both as µg of fluorescein per gram of dry mass (µg·g^{-1}) and µg of fluorescein per millilitre of liquid evaporated (µg·mL^{-1}) in Figure 7.

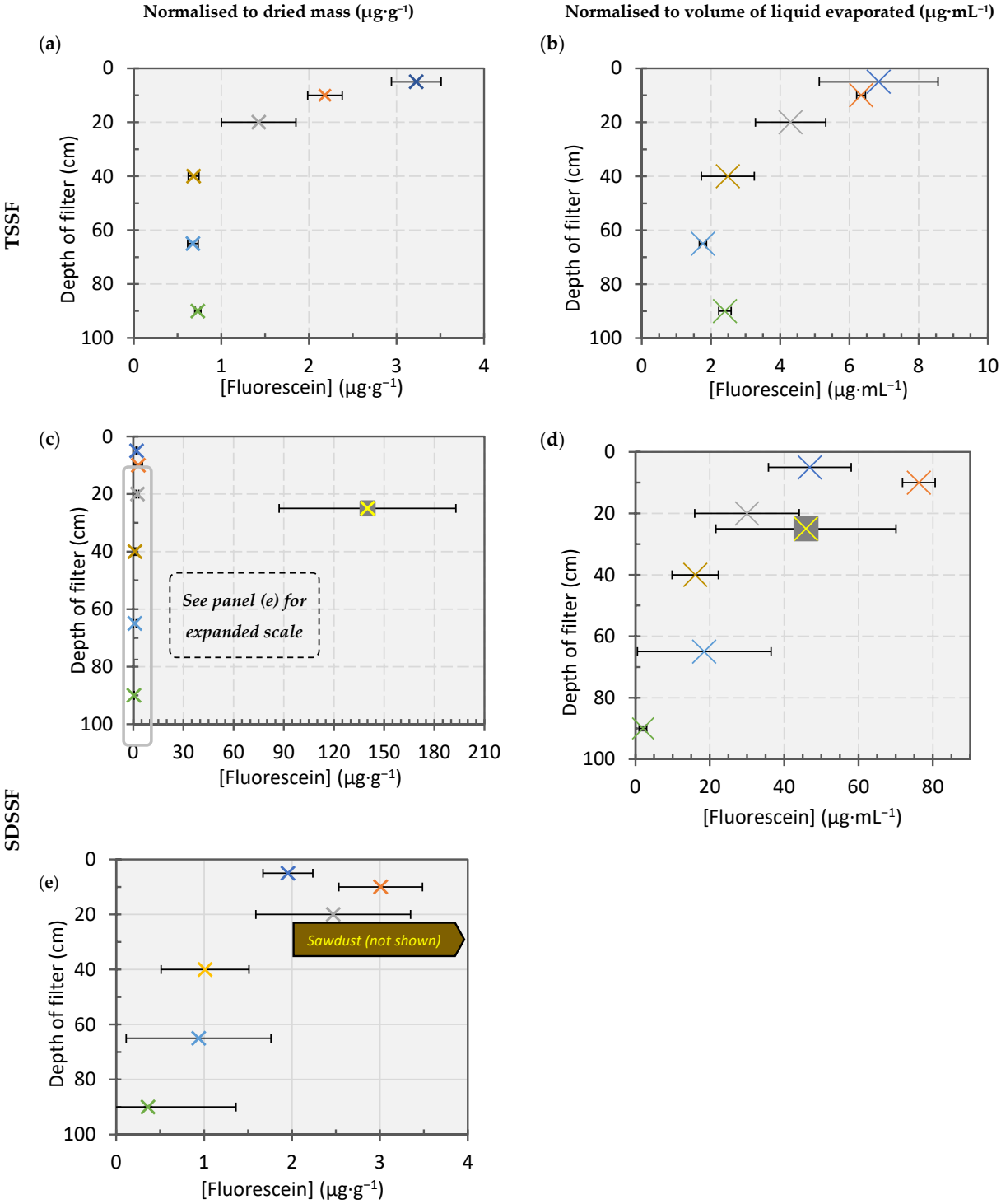


Figure 7. The enzymatic activity throughout the depth of each SSF, where (**a**,**b**) show the mean enzyme activity for each section tested for the TSSF; and (**c**–**e**) show the mean enzyme activity for each section tested for the SDSSF. 'X' markers show mean value. Note: Graph (**c**) includes all quantified depths, including the sawdust, which extended the *x*-axis; therefore, graph (**e**) is a magnified view excluding the sawdust marker to improve resolution of the data at lower concentrations.

Further individual samples of sand were analysed for microbial activity and are presented in Table 5. These samples were selected to gather data on the baseline microbial activity of sand at different time points: day 0 of operation (before introduction of the environmental samples), oven-dried, and sand from the filter columns before exposure to the SWWE containing antibiotics.

Table 5. Results from the FDA applied to three different samples of sand to gauge the baseline microbial activity in various environments.

Sample Description	Fluorescein Mean $\mu g \cdot g^{-1}$ Sample $\pm$ SD
Unused sand, air-dried	1.18 $\pm$ 0.08 (n = 2)
Unused sand, oven-dried (121 °C, 24 h)	0.21 $\pm$ 0.11 (n = 3)
Surface sand day 19 of recirculation (*TSSF*)	6.91 $\pm$ 0.03 $^{\Delta}$
Surface sand day 20 of recirculation (*SDSSF*)	6.55 $\pm$ 0.08 $^{\Delta}$

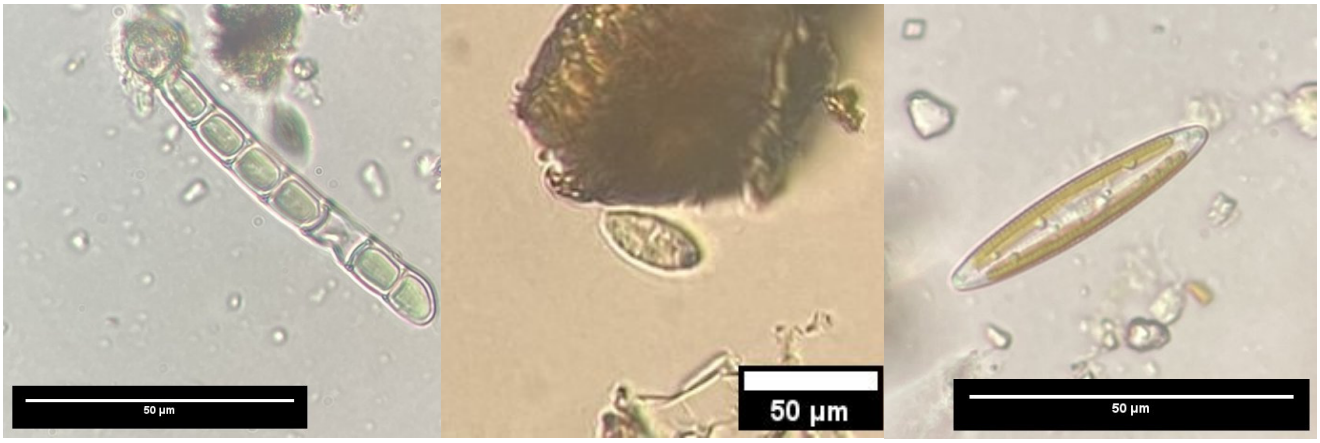
$^{\Delta}$ Due to limited amount of material for these assays, only a single assay was permitted, and thus its absorbance at 490 nm was measured in quintuplicate (technical replicates); no biological replicates were possible.

3.4.2. Microorganism Community

Table 6 outlines the microorganisms identified in the environmental feeder sample (September 2025) as well as sections of the TSSF. Exemplar images of the selected identified microorganisms are shown in Figure 8. Additional micrograph images can be found in the Supporting Information (Figure S6a–j).

Table 6. Microorganisms observed in schmutzdecke of the TSSF and September 2025 freshwater sample (bright-field microscopy, 400–1000 magnification). "X" denotes an observation of microorganisms, whereas an absence of an "X" indicates that no microorganism was observed in the sample.

Microorganism	Freshwater Sample	0–5 cm	5–10 cm	10–20 cm	20–40 cm	40–65 cm	65–90 cm
Fungi							
Hyphae		X	X	X	X		
Algae							
Diatoms	X		X		X	X	
Chlamydomonas sp.	X						
Closterium sp.		X	X				
Desmid (unidentified genus)				X			
Unidentified cyst		X					
Protozoa							
Paramecium sp.		X	X	X	X	X	X
Amoeba sp.	X				X		
Corythion sp.		X					
Helminths							
Nematode		X	X	X	X	X	
Bacteria							
Cyanobacteria	X						
Spirochaete-like	X						
Other							
Unidentified flagellate (motile)		X					
Unidentified coccoid cells (non-motile)		X	X				
Total microorganism types identified	5	8	6	4	5	3	1



(**a**) (**b**) (**c**)

Figure 8. Micrographs of (**a**) cyanobacteria (×1000 magnification), (**b**) *Paramecium* sp. (×400 magnification), and (**c**) a Navicular diatom (×1000 magnification). Each scale bar represents 50 µm.

4. Discussion

4.1. Recirculating Filters

In research settings, recirculation as an approach to filter ripening is not as common as the alternative single-pass approach. Run-to-waste SSF systems are often confined to smaller dimensions with respect to sand bed depth and surface area to reduce the quantity of water required and produced. This also enables the researcher(s) to realistically control the test variables. However, these smaller dimensions curb the tangible applications of the filter for municipal scale. Augmenting bench-scale studies to industrial magnitudes can uncover issues such as air pocket formation, loss of adsorbent, and other inefficiencies [37].

A limited number of investigations of biological filtration treatment technologies have reported a recirculation configuration in their experimental design. In one instance, a recirculation system was utilised to acclimate biofilters with an inoculant of microbial soil extract. The investigation in question [20], an up-flow biofiltration experiment utilising varying depths of activated carbon sandwiched between coarse sand, involved two modes: "acclimation" and "consecutive". It should be noted that the system was first operated in contrast to the current work, where environmental river water was fed to the up-flow filter in a consecutive mode (i.e., single-pass or run-to-waste). It was afterwards switched to a closed-loop to acclimate with a microbial community extracted from the soil. While the acclimation mode was only operated for one week, it posed as an effective way to investigate the potential of engineering microbial consortia to enhance water treatment, and isolate variables to be investigated. The investigation concluded that the composition of the microbial community within the filter exerted a greater influence on treatment performance (i.e., DOM degradation) than either the mass of activated carbon or total biomass. In parallel, the authors' experiments suggested that the localised microbial activity hotspot within the sawdust layer of the SDSSF can similarly enhance filtration performance, reinforcing the premise that microbial functionality and spatial distribution play key roles in treatment efficiency.

A recirculating biofilter was more directly investigated in 2022 by Steven et al. [19], who incorporated ceramic filter media spheres as a substrate to which biofilms could attach. An environmental sample of surface water was recirculated through a small up-flow filter (160 mm length) for a period of 4 weeks, then subjected to test pathogens *Escherichia coli*, *Enterococcus faecalis*, and *Pseudomonas aeruginosa* for 24 h recirculation. Reductions in all the indicator species were observed in the biofilters, whilst concentrations remained constant or increased in parallel sterile control filters, indicating that pathogen removal was

primarily mediated by biofilm activity. The scale and success of the system indicate suitable application where water is not for consumption, e.g., inland bathing, and longer-term storage of recycled water [38]. The filters evaluated in the present study employed an analogous biologically active recirculating configuration. Whilst the TSSF and SDSSF were investigated for their ability to remove emerging contaminants, the application is the same: biofilm-based recirculating filters have potential to control pathogens and attenuate CECs.

4.2. Environmental Freshwater

Two variables were included in the study: the inclusion of a sawdust layer in the SDSSF, and the composition of the sample introduced to each filter. While much discussion is credited to the layer of sawdust included in the SDSSF, it is noted in this section that the variation is attributed to the differing sample characteristics.

Due to high variability in the SDSSF inoculant despite triplicate analysis, the differences in concentrations of a number of parameters between the samples were determined to be not statistically significant ($p > 0.05$, two-tailed heteroscedastic *t*-test, see Table 3 for M $\pm$ SD). Nonetheless, differences were still present, markedly between phosphate levels and measured turbidity. DOM, pH, conductivity, and consequently TDS, were deemed to have significant differences between the two samples ($p < 0.05$). The subtle contrasts between each inoculant may have manifested in the differences in the operation of each filter. For example, DOM levels in the TSSF were initially elevated, with the filtrate reaching 0.4014 on day 3, before stabilising to a plateau after day 5 until the end (0.2691 $\pm$ 0.0181, Figure S4a). On the other hand, the SDSSF exhibited lower early DOM readings (0.2184 in the filtrate after day 3) followed by a steady increase over time to 0.3357 on the final day of the experiment (Figure S4b). DOM concentration of the TSSF inoculant was higher than that of the SDSSF (0.1694 vs. 0.1566, respectively); however, the subsequent trends are most likely the results of the respective microbial activities within each filter (See Section 4.3. Development of the schmutzdecke).

A similar effect was also observed in the phosphate dynamics of the SDSSF. The elevated phosphate levels were present in the SDSSF inoculant sample before concentrations stabilised and plateaued (Figure 5c). Of course, this pattern is likely influenced by dilution through recirculation and biological consumption of phosphates. Even so, it is noteworthy that systems receiving higher dosages appear to exhibit rapid stabilisation.

4.3. Development of the Schmutzdecke

4.3.1. Baseline Microbial Activity in Unused Sand

During the recirculation phase, microbial growth on the surface of the filter bed was confirmed experimentally by FDA of the samples outlined in Table 4. Unused sand from the same source, a portion of which was dried in the oven at 121 °C, was analysed and found to have a mean microbial activity of 1.18 $\mu g \cdot g^{-1}$. After almost 3 weeks of operation, these values increased to 6.91 and 6.55 $\mu g \cdot g^{-1}$ for the traditional and hybrid filters, respectively. It may be argued that this increase is perhaps the contribution of bacteria in the liquid phase in the interstitial spaces of the sample; the presence of planktonic bacteria is demonstrated in Figure 4. However, the samples were drained of as much of their liquid as possible before FDA analysis, such that the response of the assay is reflective of the recovery of microbial material attached to the sand particles by the reagent buffer. Therefore, the authors can confirm that there was an increase in bacterial activity within the filter material independent of the increase in bacteria in the recirculating phase. However, considering the oven-dried sample had a mean of 0.21 $\mu g \cdot g^{-1}$ and the unused sand had a microbial activity of 1.18 $\mu g \cdot g^{-1}$, it is also implied that the filter materials had a baseline microbial activity which may have contributed to the development of the schmutzdecke, as opposed to the

environmentally derived inoculant being the sole source of microorganisms. Given that each run utilised materials sourced from the same batch, the differences in the contribution of microbial inoculation from the sand were limited as a result. It is worth mentioning the potential here of exploiting and even engineering a bespoke community of microbiota to optimise water treatment based on the sand inoculum [39]. At the very least, pre-cultivated sand from mature SSFs can be taken advantage of to shorten the filter's ripening period [39]. This is often the case in real-world applications, where sand from deep in the filter is reused to replenish and restart a new treatment phase [15].

4.3.2. Strata of Microbial Activity Across the Filter Column

In this study, the microbial activity decreased along the depth of the filter in the TSSF (Figure 7a,b), with 77% of the total microbial activity occurring in the top 22% of the TSSF's depth (top 20 cm of sand). This finding interestingly coincides with the distribution of DO concentration observed by the authors of [31], where oxygen was gradually depleted through the depth of their filter, most significantly in the top 17.5 cm of sand. This co-location reflects the aerobic respiration of microbes consuming O_2 where labile carbon substrates have accumulated from influent waters. Since heterotrophic bacteria consume this carbon [40] like those demonstrated in both filters (Figure 4), this accumulation drives both the microbial concentration and the gradient of DO. While higher surface DO further favours the aerobic microbes, nutrient availability also appears dominant in the distribution of microbial activity [41]. Other studies utilising the FDA for enzymatic analysis in SSF also observed stratification of activity in their smaller 30 cm [29] and 40 cm [42] SSFs. Martins et al. [29] demonstrated that nutrient and DO mobility in coarse, medium, and fine sand influenced enzymatic activity, with the finer sand having limited distribution and subsequently lower microbial activity despite having retained a higher amount of DOM [29]. All the mentioned filters detected some level of microbial activity or DO in the lowest parts of their filters, highlighting that aerobic processes are possible throughout and can contribute to the removal of pathogens [41]. It is noteworthy that the microbial activity in the bottom 70 cm (20–90 cm below the sand surface) of the current study was less than that measured in the clean sand: 1.18 $\mu g \cdot g^{-1}$ (Table 5). In fact, the average microbial activity for each of the lowest 3 sections measured was 0.70 $\mu g \cdot g^{-1}$ and 1.02 $\mu g \cdot g^{-1}$ for the TSSF and SDSSF, respectively. While this diminished activity is unquestionably partly the result of exposure to SWWE with dissolved antibiotics, it further emphasises the agglomeration of biomass in the upper sections.

When comparing the two filters, fluorescein concentrations varied greatly across the sections measured in the SDSSF (Figure 7d,e), as evidenced by large standard deviations (see error bars). This variability between replicates of the same samples is indirectly a result of the greater microbial activity afforded by the sawdust layer, which had almost 50 times greater microbial activity (3 $\mu g \cdot g^{-1}$ in 5–10 cm vs. 140 $\mu g \cdot g^{-1}$ in the sawdust layer). It is hypothesised that the change in density between sand and sawdust, together with the change in tortuosity (i.e., the water flow path due to particle shape [43]), is the cause of the observed variability here. These changes in flow dynamics may have amplified small-scale heterogeneity in microbial growth and promoted the formation of biofilm "hotspots", which were detected in the random sampling for the FDA. This is in contrast to the TSSF, which demonstrated more spatially uniform conditions in the sand-only filter.

The literature reports positive relationships between bioactivity in the filter media and microbial inactivation in the filtrate [44]. Accordingly, the authors expected higher bacterial removal in the SDSSF since it demonstrated greater enzymatic, and subsequently, microbial activity. However, interestingly, the current study exhibited insignificant removal of total bacteria in the recirculating phase of the SDSSF (Figure 4b) whereas the TSSF

achieved significant removal as the schmutzdecke matured (Figure 4a). Two operational drivers for this observation are relevant. First, absolute planktonic bacteria counts in the final week of recirculation were lower in the SDSSF than the TSSF (1.78 ± 0.10 vs. 2.15 ± 0.21 Log10 CFU/mL, respectively), indicating that the SDSSF promoted inactivation of bacteria in the overflow despite negligible net removal. Second, room temperature correlated with overflow bacteria counts in opposite directions for the two systems (positive for the TSSF, negative for the SDSSF; see Supporting Information for Spearman's ranking correlation co-efficient matrix), suggesting different temperature-dependent dynamics were at play. Considering these together, these data imply that the efficiency of bacteria inactivation depends not only on the biological activity of the schmutzdecke but also on the bacteria loading concentration and environmental conditions (e.g., temperature) that govern predator–prey dynamics, as well as regrowth and sloughing of biofilm [41,43].

4.3.3. Strata of Microbial Community Across the Filter Column

The number of microorganism types identified in each section of the TSSF column decreased in a similar manner to the microbial activity (Table 6). The majority of taxa were accrued in the top 5 cm, where a total of eight types of microorganisms were observed by bright-field microscopy. Fungal hyphae were found across many of the samples, congruent with reports of fungal stratification in top layers in household SSFs [32] and full-scale SSFs [45]. The presence of the hyphae, as well as cyanobacteria (Figure 7a), is influential, as these significantly contribute to EPS production [46], and consequently schmutzdecke development.

Paramecium sp. (Figure 7b) were also prevalent throughout the filter column, indeed being observed as deep as the 65–90 cm section. Their resilient nature may facilitate their capability to biodegrade hydrocarbon residues, including polycyclic aromatic hydrocarbons (PAHs) [47], and even microplastics [48].

Algal diatoms (Figure 7c) were present sporadically within both the filter and the freshwater samples. These algae have also been noted in other wastewater treatment research [49] and are important as they produce oxygen during photosynthesis, which enhances the growth of aerobic microorganisms to further degrade contaminants [50].

Nematodes, despite being relatively larger than bacteria [32], were noted as deep as 40–65 cm below the surface of the filter (Table 6), putatively due to their high motility enabling them to penetrate deeper pore spaces [44]. These microorganisms influence the ecology of the filter by consuming bacteria, including pathogens [44], and by contributing to biofilm formation [51].

4.4. Filtrate Water Quality

4.4.1. Dissolved Oxygen

Some literature sources reported decreased DO levels in the filtrate due to consumption of oxygen by the filter's microbes for respiration and other metabolic activities, alongside oxidation reactions with the filtration material itself [49,52]. Subsequently, reaeration of the liquid phase is expected at the outlet pipe (i.e., in the filtrate) and through the water transfer pump, in the upper reservoir (not measured). In the current work, the concentration of DO in the overflow water generally tended to be higher than in the filtrate, especially during the first two weeks' operation of either filter. It can be assumed that few bacteria were colonising the filters at an early phase; the oxygen depletion observed early in both filters' operation is most likely due to alternative oxidation processes. This is substantiated in similar works, which describe the consumption of oxygen by organic content in the sand [53] as well as absorption by the pores of the filtration materials [54].

Room temperature exhibited little influence on the DO in overflow and filtrate for both filters. Although colder water can dissolve a greater amount of oxygen, a correlation co-efficient $\rho = -0.02$ (Table S3) was calculated for the overflow of the SDSSF, indicating no correlation. For the hybrid filter, the DO remained relatively stable over the experiment (overflow maintained an average of 8.32 ± 0.34 mg·L^{-1} over 33 days), only dipping to 7.36 mg·L^{-1} following the pump failure event on day 17 (see blue arrow, Figure 2b). This appears to have also had an impact on the planktonic bacterial count on day 18 (Figure 4b). Here, coupled with a very localised spike in the room temperature, proliferation of bacteria may have increased the biological demand for oxygen in the system, thus explaining the latent dip in the DO that was observed on day 20. In fact, bacterial counts were strongly associated with DO ($\rho = -1.00$, $p < 0.05$, Table S5) measured in the SDSSF overflow. However, these correlation co-efficient values should be interpreted carefully due to the limited number of bacterial count data points (n = 4); thus, the number of pair-wise observations is limited. Nonetheless, this is corroborative of the known fact that increasing aerobic processes, such as increasing the density of microorganisms, will affect the biological demand of oxygen over time [52–54].

4.4.2. Concentration of Nitrates and Phosphates

In the literature, nutrient removal efficiency often has a strong positive relationship with hydraulic retention time (HRT), which can be increased by increasing the depth of sand [43,55], as this increases the contact such pollutants have with the biological components of the SSF. Nitrifying bacteria require higher DO levels to oxidise ammonia (NH_3) to nitrate (NO_3^-) via nitrite (NO_2^-) [56]. Inversely, denitrification occurs in low-DO or anoxic microsites, transforming nitrates to nitrogen [25,43,56], e.g., deep in the filter column. Such processes can co-occur in SSF, given the DO gradient, availability of carbon, and HRT, effectively facilitating nitrate removal [55]. Ortho-phosphates, however, cannot be transformed as it is immobilised by adsorption; thus, once the SSF's capacity to retain P is reached, it will leach into the effluent [43,57]. Published work corroborates this challenge with P removal; in fact, one study could only sustain <20% removal using crushed clam shells after 10 days, and another <25% after 14 days using biochar and sand [58].

The DO trended downward over the duration of the TSSF experiment, in contrast to the SDSSF DO profile. The maximum of 9.65 mg·L^{-1} was observed in the TSSF on day 4 and a minimum of 2.72 mg·L^{-1} on day 31 (Figure 2a). This trend is strongly associated with the relative concentrations of nutrients. Here, the DO depletion correlated to increasing overflow phosphate concentration ($\rho = -0.75$, $p < 0.005$, Table S3) and phosphate and nitrate concentrations in filtrate ($\rho = -0.74$ and -0.69, respectively, both $p < 0.005$, Table S4). Since the system is a closed loop and nutrients were supplemented to the filter weekly (as outlined in Section 2.3), the increasing concentration of nutrients may partially be explained by the limited concentration of microorganisms available to consume such nutrients, i.e., the schmutzdecke was the restricting factor. Post hoc analysis of each system's filtration bed demonstrated the relative abundance of microorganisms (see Section 3.4), with the traditional filter having a relatively low microbial activity compared to the SDSSF. Given the trend in the TSSF, the plateauing of nutrient concentrations in the SDSSF system (Figure 5c,d), therefore, is likely the result of the elevated microbial activity facilitated by the sawdust layer as discussed in Section 4.3.2. The ortho-phosphate concentration in this system was highly stable. In fact, ortho-phosphate levels only exceeded 1.15 mg·L^{-1} following the pump failure event despite the weekly additions of nutrients and its environmental freshwater seeding sample containing 2.53 ± 1.15 mg·L^{-1} (3.3× as much as that added to the TSSF). This suggests that nutrient transformation processes, such as nitrification and denitrification, alongside the biological phosphorus removal, are influenced by microbial

dynamics in the filter bed. The consumption of nutrients potentially demonstrated the presence of microorganisms capable of sequestering phosphorus, namely phosphorus-accumulating organisms (PAOs) [59], although specific 16s rRNA gene sequencing should be carried out for confirmation of their presence in the filter. A recent investigation of SSF coupled with constructed wetlands also reported notable ortho-phosphate retention, reducing influent concentrations of 10.0 mg·L^{-1} to 4.0 mg·L^{-1} [60]. In that study, the authors attributed phosphorus removal primarily to adsorption onto the sand media, using a 0.25 × 0.25 m sand bed 0.25 m deep to polish the treated water. Together, these findings suggest that phosphorus attenuation in SSF-based systems may arise from both physico-chemical interactions with the filter media and biologically mediated processes within the active filter layer, with the relative contribution of each mechanism likely depending on bed composition, operating conditions, and microbial development.

In typical SSF configurations, such as that of the TSSF, microbial populations are limited by available organic carbon. The addition of sawdust thereby addresses this limitation by supplying a slow-release carbon source and enhances the activity of heterotrophic bacteria, those which consume carbon from extracellular sources [40] and were present in the overflow and filtrate of both filters (Figure 4). Such nutrient retention, given appropriate intervention and application, could substantially reduce waterway eutrophication and associated algal bloom risks [61,62].

4.4.3. Turbidity

In this work, the TSSF worked as expected, initially achieving satisfactory turbidity reductions. However, a surge in the flow rate around day 14 (Figure S1) had resuspended particulates, leading to a temporary rise in both overflow and filtrate measurements. After approximately three weeks of operation, filtrate turbidity also became unstable and, on three occasions, exceeded that of the overflow (Figure 3a). This instability coincided with a notable increase in nitrate concentration in the filtered water ($\rho = 0.53$, $p < 0.05$, Table S4). These concurrent increases suggest that schmutzdecke sloughing—biofilm shedding from the sand surface and dispersing in the liquid phase—or elevated activity of nitrifying bacteria oxidising nitrite to nitrates from within the filter may be responsible [16,56,59]. SSFs have consistently proven to be efficient for turbidity reduction, frequently meeting the World Health Organisation (WHO) guideline of 1 NTU in numerous studies [22,63,64]. Contrastingly, as with the TSSF, the operational and biological limitations can restrict performance consistency. The uniformity of material throughout the column in a traditional filter makes it highly sensitive to hydraulic disturbances [64] such as changes in loading rate observed (day 14, Figure S1). As a result, the traditional configuration may not realise its full potential without innovation.

The SDSSF, on the other hand, consistently demonstrated strong reductions in turbidity (Figure 3b), especially following the pump failure event of day 17, where the filter demonstrated capacity to cushion the spike in turbidity with a 64% removal efficiency (2.26 NTU reduced to 0.82 NTU). The literature concludes that greater turbidity removal is observed in SSF with either deeper beds or smaller particle effective size (D_{10}) [65]. While the bed depths were identical for both filters in this study, the schmutzdecke extended further down the SDSSF column (see Section 3.4.1) because of the sawdust layer inclusion. Thus, the interstitial spaces between the smaller particle sizes of the sawdust (particle sizes were found to be in the range between 0.210 and 0.300 mm), enabling greater retention and entrapment of suspended matter.

Similar to the works of Freitas et al. [49], some correlation was found between the turbidity of the TSSF filtrate and operation time ($\rho = 0.55$, $p < 0.05$, Table S4). This was also true for the same parameters within the filtrate of the SDSSF: $\rho = 0.80$ (turbidity vs.

bacterial count, Table S6) and ρ = 0.36 (turbidity vs. operation time, Table S6), although these ρ values were not deemed statistically significant. Essentially, the turbidity of the filtered water decreased over time as the filter ripened, while it has been observed that turbidity can partially predict the presence of microorganisms [63]. It should be noted that while the filtrate of both filters always achieved the World Health Organisation's (WHO) target of <1 NTU, the influent turbidity was rarely high enough to truly challenge the filter. In fact, the turbidity of the overflow only reached 1.34 and 2.26 NTU for the traditional and hybrid filters, respectively. Even these values are still considered acceptable by the WHO, which states that water quality of <5 NTU may be accepted provided a higher dose of disinfection is subsequently applied [63].

4.4.4. Conductivity and Total Dissolved Solids

The removal of particulate and suspended contamination is straightforward with SSF, as demonstrated by turbidity reductions (further discussed in Section 4.5). The changes in the concentration of dissolved matter, however, are much more complex.

In both SSFs, the conductivity generally increased over time (Figure S2). The weekly addition of nutrients to the system may have indirectly contributed to the increase in TDS as biochemical reactions ionise organic compounds and subsequently increase the total amount of dissolved ions [66]. More directly, peaks and drops in EC presented in Figure S2 also correlate with variations in nutrient concentration in the filtrate, where excess nutrient ions are being picked up by the EC probe, particularly in the EC of the TSSF's overflow, where phosphate and nitrate had ρ values of 0.80 and 0.54 ($p < 0.005$ and <0.05, respectively, Table S3). Random fluctuations are likely to be caused by the temporal effects of concentration and dilution from topping up the system with dechlorinated water, as well as the pump failure event influencing ion concentrations.

The strong correlation of the EC in overflow and filtrate in the SDSSF (ρ = 0.93, $p < 0.005$, Table S2) was absent in the TSSF (ρ = 0.43, $p > 0.05$). This is possibly due to the increased microbial activity noted in the sawdust layer, leading to an increased bacterial count (ρ = 0.92, $p < 0.05$) and DOM (ρ = 0.74, $p < 0.05$) between overflow and filtrate. In the TSSF's filtrate, the conductivity variation was isolated to the flow of excess nutrients, with ρ = −0.30 ($p > 0.05$) for bacterial count but ρ = 0.58 for DOM ($p < 0.05$).

4.4.5. The Simulated Wastewater Effluent Test

The Supplementary Information contains figures and tables relating to the challenge of the filters with SWWE. The two filter configurations demonstrated clearly different treatment profiles when challenged with the short-term SWWE test influent, indicating that the media composition strongly influenced development and performance under simulated conditions. It should be noted that the filtration rates, which are known to affect SSF treatment efficiency [13], recorded during the challenge phase were diverse: 0.21 m/h for the TSSF and 0.36 m/h for the SDSSF, potentially due to clogging of pipework and valves of the sand-only system. The sand-only TSSF achieved the greatest turbidity removal, reducing turbidity by 86 ± 7%, which suggests strong physical straining and particle retention. In contrast, the SDSSF exhibited a more moderate turbidity reduction of 45 ± 12%, and this effect was statistically detectable ($p < 0.05$, two-tailed paired *t*-test), implying that the inclusion of sawdust altered filter characteristics in a way that reduced particulate removal efficiency.

For the other parameters, both filters produced comparatively limited changes in conductivity and TDS, indicating that neither system substantially altered the concentrations of dissolved ionic load. pH was slightly decreased in both treatments, but the reduction was more pronounced in the TSSF (−7 ± 1%, $p < 0.005$) than in the SDSSF (−1 ± 0.5%),

suggesting that the sawdust layer may have buffered or moderated acid-base shifts during filtration. Dissolved oxygen responses diverged substantially: TSSF increased DO by 29 ± 17%, whereas SDSSF decreased DO by 22 ± 4% ($p < 0.05$), which may reflect greater oxygen consumption within the organic-rich sawdust layer and possible stimulation of microbial activity under more reducing conditions.

Nutrient removal also differed between systems: TSSF reduced phosphates by 40 ± 8% ($p < 0.05$), whereas SDSSF achieved a larger phosphate reduction of 63 ± 2% ($p < 0.005$) despite the greater filtration rate. This indicates that sawdust enhanced phosphate attenuation, potentially through adsorption, retention, or biologically mediated processes associated with the organic amendment facilitating greater microbial activity. Nitrate removal was highly variable in both systems, especially in the SDSSF, where the large standard deviation suggests unstable performance and weak reproducibility across replicates. DOM removal was minimal in both filters, implying that neither configuration substantially addressed dissolved organic matter under the conditions tested.

Overall, the result indicates a functional trade-off between physical remediation and nutrient removal. The sand-only filter was apparently more effective for turbidity control, while the sawdust-amended system showed stronger phosphate removal but altered reduction-oxidation-related performance, particularly evident in the DO decrease. Taken together, these findings suggest that sawdust incorporation may be advantageous where nutrient attenuation is prioritised, as well as maintaining treated water production volumes using the upper filtration rates.

4.5. Proposed Removal Mechanisms

Biologically active slow sand filters facilitate water remediation through a set of closely associated abiotic and biotic processes [43]. Primarily, contaminant molecules can be physically immobilised (sorbed and entrapped [46]) by both the surface interactions of filter material and within the schmutzdecke's biofilms [43]. Biological remediation (degradation, predation, and attenuation) then acts on these retained contaminants [6]. The synergistic action of the aforementioned mechanisms combined can, in theory, enhance the removal of even the more persistent compounds [46,67].

It should be noted that biological decay (i.e., biodegradation) is only possible with organic contaminants predominantly containing carbon–hydrogen bonds. Inorganic contaminants such as metals, metalloids, and salts cannot be biodegraded and therefore require SSF modifications that promote their immobilisation (e.g., via sorption) until the available capacity is exhausted, and the materials are replaced to prevent leaching of the contaminants back into the effluent [64,68]. The focal point of several studies surrounding the remediation of water from emerging contaminants is on the development of novel sorption materials such as amending biochar [68] with iron oxides [62,69].

Studying the surface of the filtration materials can help to explain the mechanisms of removal within an SSF. The surface charge of an adsorbent is a balance of positive and neutral charges [70], and is dependent on the surrounding pH (wastewater effluent is circumneutral, i.e., ~pH 7 [26]). In the same way, the acid dissociation constants of the contaminating compounds (pK_a = 7.12 and 5.7, for TMP and SMX, respectively [71,72]) can also influence their electric charge and the interactions with the adsorbent material [70,73]. Electrostatic interactions between the adsorbent (filter material) and solute (contaminant) can strongly favour adsorption and thus, the removal of contaminants. Conversely, like-charge repulsion hinders adsorption [11,74]. However, the removal process goes beyond that; it often is a combination of numerous processes: ion exchange, hydrogen bonding, hydrophobic interactions, π–π interactions, and biodegradation [12,74,75].

Although TMP removal was consistently high in this short once-through experiment, it is uncertain whether this level would be maintained during prolonged operation. Our study captured only a single-day exposure rather than the longer-term performance observed in continuous filtration studies, and as such, some adsorption capacity may have remained in the sand matrix of both filters. Over time, removal may decline as the available adsorption sites become saturated [43]; however, the modified sawdust in the SDSSF may offer additional adsorptive capacity [76] and could support improved performance during longer-term operation. The authors plan to explore this next within the ongoing study.

In comparison, an investigation of an anaerobic membrane bioreactor reported a 97% removal of TMP by activated sludge where the starting concentration was 150 $\mu g \cdot L^{-1}$ [77]. The same investigation also demonstrated poor SMX removal through batch adsorption tests; low adsorption of the negatively charged compound to the negatively charged biomass resulted in less than 15% removal [77]. This corresponded to the current experiments where SMX was removed in TSSF by on average 14.5 $\pm$ 20.9% of SMX, and SDSSF removed 2.3 $\pm$ 1.0%. The large variation in SMX removal observed in the TSSF was driven largely by a single replicate with 38.6% removal, whereas the median removal across the entire run was only 3.7%, indicating that typical performance was close to zero removal.

Published batch studies confirm that, unlike TMP removal, SMX removal by adsorption is largely independent of contact time but strongly pH-dependent [74,75]. This is consistent with the findings from our large-scale SWWE challenge. Since pH and contact time were identical across both filters in this study, the consistently low removal level of SMX suggests electrostatic repulsion between the anionic SMX species (negatively charged) and neutrally charged surfaces of both sand and sawdust. Published studies demonstrating SMX removal indicate that its elimination is largely driven by biodegradation, a relatively slow, rate-limiting process that requires an acclimated microbial community. In activated sludge reactors, an alternative biological treatment approach, substantial SMX removal was only achieved after several days of acclimation (in the order of 2–4 days), highlighting the importance of sufficient contact time with biological decay [77]. In the present study, the filter operated in run-to-waste mode during the challenge, which likely provided insufficient hydraulic residence time (estimated 1–2 h, unpublished data) for microbial adaptation to the simulated water and for development of an active SMX-degrading biofilm.

Also in this investigation, TMP removal is consistent with adsorption being the major removal pathway, whereas the poor and highly variable SMX removal suggests limited sorption under the tested conditions and insufficient residence time for meaningful biological degradation. Importantly, the sawdust layer should be considered separately from the schmutzdecke: it is a distinct reactive media layer that may contribute additional sorptive capacity and alter hydraulic flow paths, while the schmutzdecke represents the biologically colonised surface zone that develops across the filter bed (see Section 3.4, Strata of the filter column). A recirculating filter configuration could therefore improve removal of persistent contaminants such as SMX. By effectively increasing residence time, biofilm interactions and biodegradation capacities are both promoted, to which SMX is susceptible [69,75]. This will form part of the future work at Ulster University.

5. Conclusions and Recommendations

The research presented in this paper outlines the particulars of SSF and the effect of incorporating a treated sawdust as a novel filter material with enhanced adsorption attributes. The investigation involved recirculating the SSF effluent through the filter over several weeks to support the development of a stable, consistent schmutzdecke biofilm layer.

During the experiments with simulated wastewater effluents, both filters demonstrated high removal rates of trimethoprim (93.4% and 98.6% for the TSSF and SDSSF, respectively), while the sulfamethoxazole removal remained modest at best (<38.6% in both), thus highlighting the compound-specific nature of contaminant attenuation in SSF systems previously considered. Additionally, the SDSSF configuration was shown to reduce ortho-phosphate concentration in the short-term performance testing, with an average removal of 62.6 ± 2.1%, whereas the TSSF removed 39.5 ± 8.3% (Table S7). Collectively, these findings indicate that recirculating SSF systems provide a robust and resource-efficient platform for studying biofilm-mediated treatment processes at meaningful scales. The incorporation of low-cost, waste-derived lignocellulosic materials also suggests potential relevance for decentralised treatment contexts, including rural areas and small communities, where simple, low-energy technologies are often preferred. However, further long-term pilot-scale studies are required to confirm cost-effectiveness, scalability, and operational stability under real-world conditions.

Although the sawdust-amended filter showed enhanced phosphate removal, its long-term operational stability remains uncertain. As an organic material, sawdust may progressively degrade during extended use, potentially releasing organic compounds which were sorbed onto the material's surface, altering pore structure, and reducing hydraulic conductivity. Degradation of the material was not visually observed in the current study, and the sawdust amendment may actually increase the removal capacity as discussed before. Still, long-term column studies are needed to evaluate the likelihood of clogging, the effective service life of the filter, and maintenance intervals.

This study demonstrates the practicability of operating a pilot-scale recirculating down-flow slow sand filter to promote controlled development of the schmutzdecke while minimising water consumption, hence adopting a sustainable design ethos. The configuration supported microbial colonisation and stable biofilm formation, as evidenced by increases in enzymatic activity and microbial diversity within the filtration bed. Incorporation of a treated lignocellulosic layer derived from sawdust enhanced the microbial activity at depth and improved several aspects of filter performance, including more stable turbidity removal, which consistently achieved WHO targets of <1 NTU. The additional layer also attenuated nutrients during recirculation, maintaining filtrate ortho-phosphate levels ca. 1.09 $mg \cdot L^{-1}$. Nitrate concentrations also remained low during much of the experiment, although levels appear to increase towards the end (Figure 5d). With its highest filtrate concentration of 2.1 $mg \cdot L^{-1}$, the SDSSF appears to out-perform the TSSF with respect to nitrate reduction, which peaked at 4.7 $mg \cdot L^{-1}$. The microbial density of the filtrate produced by the filter containing sawdust did increase over the duration of the experiment; however, this may be ameliorated through further disinfection processes.

An untapped potential is therefore presented: what if wastewater effluent containing emerging contaminants is recirculated in batch fashion? In practical terms, this might look like configuring multiple treatment columns in series to increase and industrialise the volumes of treated water possible. Incorporation of a recirculating filter unit before more sensitive treatment processes could also reduce the contaminant loading on downstream systems, as is common in typical wastewater treatment designs.

Future work should further characterise contaminant-sawdust adsorption processes and investigate long-term operational stability to better understand the mechanisms governing contaminant removal. Molecular approaches such as 16s rRNA or nested PCR could also be incorporated to identify microbial community composition and better attribute microbiological treatment mechanisms. From a practical perspective, future studies should also evaluate the scalability, maintenance requirements, and cost-effectiveness of sawdust-

amended slow sand filtration systems, while challenging them with a broader range of contaminants to assess treatment resilience under real-world operating conditions.

Supplementary Materials: The following supporting information can be downloaded at https://www.mdpi.com/article/10.3390/separations13070201/s1: Text S1: Manufacture, operation, and monitoring procedures; Table S1: Traditional slow sand filter correlation co-efficient values, overflow vs. filtrate parameters; Table S2: Sawdust slow sand filter correlation co-efficient values, overflow vs. filtrate parameters; Table S3: Traditional slow sand filter inter-parameter correlation co-efficient values - overflow; Table S4: Traditional slow sand filter inter-parameter correlation co-efficient values - filtrate; Table S5: Sawdust slow sand filter inter-parameter correlation co-efficient values - overflow; Table S6: Sawdust slow sand filter inter-parameter correlation co-efficient values - filtrate; Table S7: Average change in each parameter in SWWE challenge; Figure S1: Flow rates measured at the overflow and filtrate outlets of the (a) Traditional SSF, and (b) Sawdust SSF; Figure S2: Conductivity in the overflow and filtrate of the (a) Traditional SSF, and (b) Sawdust SSF; Figure S3: pH of overflow and filtrate for the (a) traditional SSF, and (b) Sawdust SSF, with inset graphs to show minute pH changes; Figure S4: The absorbance of ultraviolet (UV) radiation at wavelength 254 nm for the overflow and filtrate of the (a) Traditional SSF, and (b) Sawdust SSF; Figure S5: Side-by-side comparison of filter performance across a range of parameters for TSSF (a, c, e, g, i , and k) and SDSSF (b, d, f, h, j, and l); Figure S6: Selected images photographed from bright-field microscopy, subjects and scale bars of each are noted in individual captions.

Author Contributions: Conceptualisation and methodology, H.C., B.S., S.T.-M., P.F.-I. and B.L.S.F.; resources, R.M.; writing—original draft preparation, H.C.; writing—review and editing, H.C., B.S., S.T.-M. and P.F.-I.; supervision, B.L.S.F., S.T.-M., P.F.-I. and R.M. All authors have read and agreed to the published version of the manuscript.

Funding: This research received no external funding.

Data Availability Statement: The original contributions presented in this study are included in the article/Supplementary Materials. Further inquiries can be directed to the corresponding author.

Acknowledgments: This work was supported by a postgraduate studentship awarded by the Department for the Economy (DfE) of Northern Ireland, and funding supplied by Jayanta Mondol within BSABE, for the manufacture of the filter apparatus. Sand materials were acquired from Noel Mongan (Ballyshannon WTP). The authors gratefully acknowledge the efforts of Mark Wilson within BSABE, for the technical expertise and manufacture of the filtration apparatus, together with Frederick Akpomie for assistance in sample collection and maintenance of the system.

Conflicts of Interest: The authors declare no conflicts of interest.

Abbreviations

The following abbreviations are used in this manuscript:

AC	Activated carbon
AOP	Advanced oxidation process
C	Carbon
CEC	Contaminants of emerging concern
cm	Centimetre
C_U	Co-efficient of uniformity
BSABE	Belfast School of Architecture and the Built Environment
D_{10}	In particle size analysis, the diameter at which 10% of the sample is finer
D_{60}	In particle size analysis, the diameter at which 60% of the sample is finer
DfE	Department for the Economy
DOM	Dissolved organic matter
EPS	Extracellular polymeric substance
FDA	Fluorescein diacetate

HPLC	High-performance liquid chromatography
SDSSF	Hybrid slow sand filtration
kg	Kilogram
L	Litre
LEV	Local exhaust ventilation
M	Mean
mg	Milligram
mL	Millilitre
µg	Microgram
µm	Micrometre
mm	Millimetre
nm	Nanometre
N	Nitrogen
NO_3^-	Nitrates
NTU	Nephelometric turbidity unit
P	Phosphorus
pK_a	Acid dissociation constant
PO_4^{3-}	ortho-Phosphates
PPCPs	Pharmaceuticals and personal care products
PVC	Polyvinyl chloride
SD	Standard deviation
SI	Supporting information
SiO_2	Silicon dioxide or silica
SMX	Sulfamethoxazole
SSF	Slow sand filter or slow sand filtration
SWWE	Simulated wastewater effluent
TMP	Trimethoprim
TSA	Tryptone soya agar
TSSF	Traditional slow sand filter
UV	Ultraviolet
WHO	World Health Organisation
WTP	Water Treatment Plant

References

1. Kuzma, S.; Bierkens, M.F.; Lakshman, S.; Luo, T.; Saccoccia, L.; Sutanudjaja, E.H.; Van Beek, R. *Aqueduct 4.0: Updated Decision-Relevant Global Water Risk Indicators*; World Resources Institute: Washington, DC, USA, 2023. [CrossRef]
2. Jones, E.R.; Bierkens, M.F.P.; Wanders, N.; Sutanudjaja, E.H.; van Beek, L.P.H.; van Vliet, M.T.H. Current wastewater treatment targets are insufficient to protect surface water quality. *Commun. Earth Environ.* **2022**, *3*, 221. [CrossRef]
3. Brady, J.; Gray, N.F. Reform of the Irish water sector: Opportunities and challenges. *Proc. Inst. Civ. Eng. Water Manag.* **2016**, *170*, 165–174. [CrossRef]
4. United Nations. SDG 6 Data Portal. 2025. Available online: https://www.sdg6data.org/en (accessed on 10 December 2025).
5. Undp, E. *A Matter of Choice: People and Possibilities in the Age of AI*; Human Development Report, no. 2025; United Nations: New York, NY, USA, 2025.
6. Corbett, H.; Solan, B.; Tretsiakova-McNally, S.; Fernandez-Ibañez, P.; McDermott, R. New Wine in Old Bottles: The Sustainable Application of Slow Sand Filters for the Removal of Emerging Contaminants, a Critical Literature Review. *Sustainability* **2024**, *16*, 10595. [CrossRef]
7. European Parliament and Council of the European Union. Directive (EU) 2024/3019 of 27 November 2024 concerning urban wastewater treatment (recast). *Off. J. Eur. Union* **2024**, *2024*, 1–59.
8. Rapp-Wright, H.; Regan, F.; White, B.; Barron, L.P. A year-long study of the occurrence and risk of over 140 contaminants of emerging concern in wastewater influent, effluent and receiving waters in the Republic of Ireland. *Sci. Total Environ.* **2023**, *860*, 160379. [CrossRef] [PubMed]
9. Sousa, E.M.L.; Otero, M.; Gil, M.V.; Ferreira, P.C.S.; Esteves, V.I.; Calisto, V. Insights into matrix and competitive effects on antibiotics removal from wastewater by activated carbon produced from brewery residues. *Environ. Technol. Innov.* **2023**, *30*, 103074. [CrossRef]

10. Li, J.; Zhou, Q.; Campos, L.C. The application of GAC sandwich slow sand filtration to remove pharmaceutical and personal care products. *Sci. Total Environ.* **2018**, *635*, 1182–1190. [CrossRef] [PubMed]
11. Akinsanmi, O.; Kaya, S.; Tretsiakova-McNally, S.; Arnscheidt, J.; Altayan, M.; Coleman, H. Tackling Antimicrobial Resistance: Adsorption of meropenem and ciprofloxacin on ligno-cellulosic substrate from sawdust. In Proceedings of the European Waste Water Management Conference, Telford, UK, 16 July 2019. Available online: https://pure.ulster.ac.uk/en/publications/tackling-antimicrobial-resistance-adsorption-of-meropenem-and-cip/ (accessed on 5 October 2023).
12. Harmayani, K.D.; Anwar, A.H.M.F. Adsorption kinetics and equilibrium study of nitrogen species onto radiata pine (*Pinus radiata*) sawdust. *Water Sci. Technol.* **2016**, *74*, 402–415. [CrossRef] [PubMed]
13. Li, N.; Li, X.; Zhao, L.; Lu, Z.-D.; Liu, Y.-W.; Wang, N. Slow sand filters with variable filtration rates for rainwater purification: Microecological differences between biofilm and water phases. *J. Environ. Manag.* **2025**, *375*, 124210. [CrossRef] [PubMed]
14. Kotsia, D.; Lykourinas, N.; Fountoulakis, M.S. Performance of a pilot hybrid constructed wetland–sand filter system for treating dairy wastewater in a small dairy industry. *J. Water Process Eng.* **2025**, *79*, 109040. [CrossRef]
15. Higgins, K.; McBratney, D.; Ní Eidhin, C.; Page, D.; Minihan, M.; Campbell, R.; Fitzgerald, J.; Breen, D.; MacDonald, B.; Gallagher, J.; et al. *Water Treatment Manual: Filtration*; Environmental Protection Agency: Dublin, Ireland, 2020. Available online: https://www.epa.ie/publications/compliance--enforcement/drinking-water/advice--guidance/EPA-Water-Filtration-Manual.pdf (accessed on 5 October 2023).
16. Bun, S.; Chawaloesphonsiya, N.; Ermukdakul, T.; Pungrasmi, W.; Suwannasilp, B.B.; Painmanakul, P. Suspended solid and nitrate removal from aquaculture system wastewater by different approaches. *Desalin. Water Treat.* **2017**, *81*, 87–94. [CrossRef]
17. Hashmi, Z.; Metali, F.; Amin, M.; Abu Bakar, M.S.; Wibisono, Y.; Nugroho, W.A.; Bilad, M.R. Recirculating aquaculture systems: Advances, impacts, and integrated pathways for sustainable growth. *Bioresour. Technol. Rep.* **2025**, *32*, 102340. [CrossRef]
18. Li, Z.; Zhang, C.; Su, P.; Zhao, G.; Wang, Z.; Li, Y.; Li, Y.; Wang, M.; Qiao, P.; Guo, J.; et al. The feasibility and prospects of coal mine water as a cooling medium for data centers. *J. Environ. Chem. Eng.* **2025**, *13*, 117365. [CrossRef]
19. Steven, J.A.C.; Thorn, R.M.S.; Robinson, G.M.; Turner, D.; Lee, J.E.; Reynolds, D.M. The control of waterborne pathogenic bacteria in fresh water using a biologically active filter. *npj Clean Water* **2022**, *5*, 30. [CrossRef]
20. Huang, F.; Graham, N.J.D.; Su, Z.; Xu, L.; Yu, W. Capabilities of Microbial Consortia from Disparate Environment Matrices in the Decomposition of Nature Organic Matter by Biofiltration. *Water Res.* **2024**, *262*, 122047. [CrossRef] [PubMed]
21. CAWST. *Biosand Filter Construction Manual*; Centre for Affordable Water and Sanitation Technology: Calgary, AB, Canada, 2012. Available online: www.cawst.org (accessed on 11 August 2025).
22. Freitas, B.L.S.; Terin, U.; Fava, N.; Maciel, P.; Garcia, L.; Medeiros, R.; Oliveira, M.; Fernandez-Ibañez, P.; Byrne, J.; Sabogal-Paz, L. A critical overview of household slow sand filters for water treatment. *Water Res.* **2022**, *208*, 117870. [CrossRef] [PubMed]
23. *BS EN 933-2:2020*; Tests for Geometrical Properties of Aggregates—Determination of Particle Size Distribution. Test Sieves, Nominal Size of Apertures. BSI: London, UK, 2020.
24. Desmond, P.; Best, J.P.; Morgenroth, E.; Derlon, N. Linking composition of extracellular polymeric substances (EPS) to the physical structure and hydraulic resistance of membrane biofilms. *Water Res.* **2018**, *132*, 211–221. [CrossRef] [PubMed]
25. Tian, L.; Wang, L.; Zhang, X.; Huang, X.; Wang, F.; Zhu, S.; Li, X.; Guan, Y. Multi-omics analysis on seasonal variations of the biofilm microbial community in a full-scale pre-denitrification biofilter. *Environ. Sci. Pollut. Res.* **2023**, *30*, 24284–24298. [CrossRef] [PubMed]
26. Tolosana-Moranchel, A.; McMichael, S.; Hamilton, J.W.J.; Byrne, J.A.; Fernández-Ibañez, P. Electrochemically assisted photocatalytic degradation of contaminants of emerging concern in simulated wastewater using WO3—Elucidation of mechanisms. *Chem. Eng. J.* **2023**, *458*, 141442. [CrossRef]
27. Adil, S.; Maryam, B.; Kim, E.; Dulova, N. Individual and simultaneous degradation of sulfamethoxazole and trimethoprim by ozone, ozone/hydrogen peroxide and ozone/persulfate processes: A comparative study. *Environ. Res.* **2020**, *189*, 109889. [CrossRef] [PubMed]
28. Adam, G.; Duncan, H. Development of a sensitive and rapid method for the measurement of total microbial activity using fluorescein diacetate (FDA) in a range of soils. *Soil Biol. Biochem.* **2001**, *33*, 943–951. [CrossRef]
29. Martins, M.; Lunardi, S.; Puhl, V.D.A.; Pizzolatti, B.S.; Soares, M. Enzymatic analysis in bank filtration sites as a tool for assessing biological clogging—A column study. *J. Water Process Eng.* **2021**, *44*, 102375. [CrossRef]
30. Schneider, C.A.; Rasband, W.S.; Eliceiri, K.W. NIH Image to ImageJ: 25 years of image analysis. *Nat. Methods* **2012**, *9*, 671–675. [CrossRef] [PubMed]
31. Freitas, B.L.S. Filtros Lentos Domiciliares Com Operação Contínua Como Alternativa Para Sistemas de Tratamento de Águas Superficiais em Comunidades Isoladas: Uma Avaliação Comparativa Para Redução do Leito filtrante. Ph.D. Thesis, Universidade de São Paulo, São Paulo, Brazil, 2021.
32. Fava, N.D.M.N.; Terin, U.C.; Freitas, B.L.S.; Sabogal-Paz, L.P.; Fernandez-Ibañez, P.; Byrne, J.A. 'Household Slow Sand Filters in Continuous and Intermittent Flows and their Efficiency in Microorganism's removal from River Water. *Environ. Technol.* **2020**, *43*, 1583–1592. [CrossRef]

33. Rusydi, A.F. Correlation Between Conductivity and Total Dissolved Solid in Various Type of Water: A Review. *IOP Conf. Ser. Earth Environ. Sci.* **2018**, *118*, 012019. [CrossRef]
34. American Public Health Association. *Standard Methods for the Examination of Water and Wastewater*, 24th ed.; American Public Health Association: Washington, DC, USA, 2017.
35. Tolosana-Moranchel, A.; Pichel, N.; Lubarsky, H.; Byrne, J.A.; Fernández-Ibañez, P. Photoelectrocatalytic degradation of pharmaceuticals and inactivation of viruses in water with tungsten oxide electrodes. *J. Environ. Chem. Eng.* **2022**, *10*, 107955. [CrossRef]
36. Chopyk, J.; Nasko, D.J.; Allard, S.; Bui, A.; Pop, M.; Mongodin, E.F.; Sapkota, A.R. Seasonal dynamics in taxonomy and function within bacterial and viral metagenomic assemblages recovered from a freshwater agricultural pond. *Environ. Microb.* **2020**, *15*, 18. [CrossRef] [PubMed]
37. Rajandran, P.; Masngut, N.; Manas, N.H.A.; Azelee, N.I.W.; Fuzi, S.F.Z.M.; Bunyamin, M.A.H. Fixed-bed adsorption for industrial wastewater purification: An in-depth review. *Int. J. Environ. Sci. Technol.* **2025**, *22*, 3943–3964. [CrossRef]
38. Steven, J.A.C. The Development of Small-Scale, Low-Cost Biofilm Treatment Systems for the Control of Pathogens in Fresh Water. Ph.D. Thesis, University of the West of England, Bristol, UK, 2023.
39. Rosenqvist, T.; Chan, S.; Ahlinder, J.; Salomonsson, E.N.; Suarez, C.; Persson, K.M.; Rådström, P.; Paul, C.J. Inoculation with adapted bacterial communities promotes development of full scale slow sand filters for drinking water production. *Water Res.* **2024**, *253*, 121203. [CrossRef] [PubMed]
40. Allen, M.J.; Edberg, S.C.; Reasoner, D.J. Heterotrophic plate count bacteria—What is their significance in drinking water? *Int. J. Food Microbiol.* **2004**, *92*, 265–274. [CrossRef] [PubMed]
41. Trikannad, S.A.; Van Halem, D.; Foppen, J.W.; Van Der Hoek, J.P. The contribution of deeper layers in slow sand filters to pathogens removal. *Water Res.* **2023**, *237*, 119994. [CrossRef] [PubMed]
42. Puhl, V.A.; Martins, M.; Lunardi, S.; Pizzolatti, B.; Toebe, M.; Decezaro, S.; Medeiros, R.; Soares, M. Enzymatic analysis in household intermittent slow sand filters as a tool for assessing biological clogging. *J. Water Process Eng.* **2023**, *55*, 104177. [CrossRef]
43. Welz, P.J. Biosand Reactors for Municipal and Industrial Wastewater Treatment: Status Quo, Challenges and Opportunities. *Processes* **2024**, *12*, 641. [CrossRef]
44. Bai, X.; Samari-Kermani, M.; Schijven, J.; Muyzer, G.; Dinkla, I.J.T.; Raoof, A. Schmutzdecke maturation and layers' contribution to bacterial removal performance in slow sand filters for drinking water production. *Water Res.* **2026**, *298*, 125716. [CrossRef] [PubMed]
45. Rosenqvist, T.; Chan, S.; Paul, C.J. Uncharacterized members of the phylum Rozellomycota dominate the fungal community of a full-scale slow sand filter for drinking water production. *Water Res.* **2025**, *279*, 123447. [CrossRef] [PubMed]
46. Gadd, G.M. Metals, minerals and microbes: Geomicrobiology and bioremediation. *Microbiology* **2010**, *156*, 609–643. [CrossRef] [PubMed]
47. Kachieng'a, L.; Momba, M.N.B. The synergistic effect of a consortium of protozoan isolates (*Paramecium* sp., *Vorticella* sp., *Epistylis* sp. and *Opercularia* sp.) on the biodegradation of petroleum hydrocarbons in wastewater. *J. Environ. Chem. Eng.* **2018**, *6*, 4820–4827. [CrossRef]
48. Nugroho, F.A.; Fyda, J. Uptake of plastic microbeads by ciliate *Paramecium aurelia*. *Sci. Technol. Innov.* **2020**, *9*, 1–9. [CrossRef]
49. Freitas, B.L.S.; Terin, U.C.; Fava, N.d.M.N.; Sabogal-Paz, L.P. Filter media depth and its effect on the efficiency of Household Slow Sand Filter in continuous flow. *J. Environ. Manag.* **2021**, *288*, 112412. [CrossRef] [PubMed]
50. Marella, T.K.; López-Pacheco, I.Y.; Parra-Saldívar, R.; Dixit, S.; Tiwari, A. Wealth from waste: Diatoms as tools for phycoremediation of wastewater and for obtaining value from the biomass. *Sci. Total Environ.* **2020**, *724*, 137960. [CrossRef] [PubMed]
51. Đurin, B.; Alamatian, E.; Ramezani, M.; Dadar, S.; Nakić, D. Enhanced Nematode Reduction in Drinking Water Using Sodium Hypochlorite and Ozone. *Water* **2025**, *17*, 2148. [CrossRef]
52. Lubarsky, H.; Fava, N.d.M.N.; Freitas, B.L.S.; Terin, U.C.; Oliveira, M.; Lamon, A.W.; Pichel, N.; Byrne, J.A.; Sabogal-Paz, L.P.; Fernandez-Ibañez, P. Biological Layer in Household Slow Sand Filters: Characterization and Evaluation of the Impact on Systems Efficiency. *Water* **2022**, *14*, 1078. [CrossRef]
53. Zeeshan, M.; Klitzke, S.; Ruhl, A.S. Changes in dissolved organic matter and oxygen consumption in different bank filtration simulations at different scales. *Environ. Sci. Water Res. Technol.* **2023**, *9*, 1862–1869. [CrossRef]
54. Kaiser, T.; Acevedo Alonso, V.; Fundneider, T.; Lackner, S. The significance of granular activated carbon pore structure in modeling dissolved organic carbon removal in fixed-bed filters. *Chem. Eng. J.* **2023**, *464*, 142729. [CrossRef]
55. Nakhla, G.; Farooq, S. Simultaneous nitrification-denitrification in slow sand filters. *J. Hazard. Mater.* **2003**, *96*, 291–303. [CrossRef] [PubMed]
56. Zhang, S.; Huang, Y.; Ding, J.; Wang, X.; Li, R.; Li, S.; Zhang, L. Insights into the role of extracellular polymeric substances in ciprofloxacin and sulfamethoxazole removal in partial denitrification system. *J. Environ. Chem. Eng.* **2026**, *14*, 120929. [CrossRef]
57. Hamisi, R.; Renman, A.; Renman, G.; Wörman, A.; Thunvik, R. Long-term phosphorus sorption and leaching in sand filters for onsite treatment systems. *Sci. Total Environ.* **2022**, *833*, 155254. [CrossRef] [PubMed]

58. Emslie, D.; Siddiqua, S.; Crawford, B.; Teece, W. Biofilm Formation and Effectiveness of Biosand Filtration Systems with Typical and Innovative Filter Media. *Geotech. Geol. Eng.* **2022**, *40*, 1251–1266. [CrossRef]
59. Papp, L.A.; Cardinali-Rezende, J.; Júdice, W.A.d.S.; Sanchez, M.B.; Araújo, W.L. Low biological phosphorus removal from effluents treated by slow sand filters. *Appl. Microbiol. Biotechnol.* **2022**, *106*, 5797–5809. [CrossRef] [PubMed]
60. Benyagoub, M.; Fellah, A.C.; Khelladi, R.M.B.; Cherif, L.; Fellah, F.Z.C.; Boulefred, S.; Benadda, L. Performance of Phragmites Australis and Slow Sand Filtration in a Multi-Stage Vertical Constructed Wetland for Enhanced Domestic Sewage Treatment. *Water Air Soil Pollut.* **2026**, *237*, 912. [CrossRef]
61. Reid, N.; Reyne, M.I.; O'nEill, W.; Greer, B.; He, Q.; Burdekin, O.; McGrath, J.W.; Elliott, C.T. Unprecedented Harmful algal bloom in the UK and Ireland's largest lake associated with gastrointestinal bacteria, microcystins and anabaenopeptins presenting an environmental and public health risk. *Environ. Int.* **2024**, *190*, 108934. [CrossRef] [PubMed]
62. Cai, R.; Wang, X.; Ji, X.; Peng, B.; Tan, C.; Huang, X. Phosphate reclaim from simulated and real eutrophic water by magnetic biochar derived from water hyacinth. *J. Environ. Manag.* **2017**, *187*, 212–219. [CrossRef] [PubMed]
63. Cameron, J.; World Health Organization (Eds.) *Valuing Water, Valuing Livelihoods: Guidance on Social Cost-Benefit Analysis of Drinking-Water Interventions, with Special Reference to Small Community Water Supplies*; IWA Publishing: London, UK; World Health Organization: New York, NY, USA, 2011.
64. Maiyo, J.K.; Dasika, S.; Jafvert, C.T. Slow Sand Filters for the 21st Century: A Review. *Int. J. Environ. Res. Public Health* **2023**, *20*, 1019. [CrossRef] [PubMed]
65. King-Nyamador, G.; Amoatey, P.K.; Amoah, S.; Adu-Ampong, B. Optimal bed thickness and effective size for improving wastewater quality for irrigation. *Int. J. Energy Environ. Eng.* **2021**, *12*, 175–190. [CrossRef]
66. Chibueze, C.V.; Nnaji, C.C.; Mama, C.N.; Nwankwo, E.J. Integrated treatment of stormwater using multistage filtration (MSF) for domestic application (reuse). *Water SA* **2024**, *50*, 154–165. [CrossRef]
67. Ohore, O.E.; Qin, Z.; Sanganyado, E.; Wang, Y.; Jiao, X.; Liu, W.; Wang, Z. Ecological impact of antibiotics on bioremediation performance of constructed wetlands: Microbial and plant dynamics, and potential antibiotic resistance genes hotspots. *J. Hazard. Mater.* **2022**, *424*, 127495. [CrossRef] [PubMed]
68. Mohan, D.; Sarswat, A.; Ok, Y.S.; Pittman, C.U. Organic and inorganic contaminants removal from water with biochar, a renewable, low cost and sustainable adsorbent—A critical review. *Bioresour. Technol.* **2014**, *160*, 191–202. [CrossRef] [PubMed]
69. Muzawazi, E.S.; Thusabantu, N.; Oluwalana-Sanusi, A.E.; Mukaratirwa-Muchanyereyi, N.; Mamba, G.; Mokoena, P.; Mabuba, N.; Chaukura, N. Surface-loaded Fe_2O_3-biochar for the abatement of antibiotics from pharmaceutical wastewater. *Int. J. Environ. Sci. Technol.* **2024**, *21*, 3827–3844. [CrossRef]
70. Bakatula, E.N.; Richard, D.; Neculita, C.M.; Zagury, G.J. Determination of point of zero charge of natural organic materials. *Environ. Sci. Pollut. Res.* **2018**, *25*, 7823–7833. [CrossRef] [PubMed]
71. Trimethoprim (Compound). PubChem. Available online: https://pubchem.ncbi.nlm.nih.gov/compound/Trimethoprim (accessed on 9 March 2026).
72. Sulfamethoxazole (Compound). PubChem. Available online: https://pubchem.ncbi.nlm.nih.gov/compound/Sulfamethoxazole (accessed on 9 March 2026).
73. Ashadullah, A.K.M.; Kishimoto, N. Effectiveness of active control of surface charge of filter media on separation of microparticles from contaminated wastewater. *Appl. Water Sci.* **2018**, *8*, 231. [CrossRef]
74. Carneiro, R.B.; Takeda, P.Y.; Dias, M.E.S.; Nogueira, E.W.; Zaiat, M.; Santos-Neto, Á.J. Biosorption assessment of emerging contaminants onto acidogenic and methanogenic biofilm reactors: Influence of lipophilic and electrostatic interactions. *J. Environ. Chem. Eng.* **2025**, *13*, 115654. [CrossRef]
75. Stylianou, M.A.; Christou, A.; Michael, C.; Agapiou, A.; Papanastasiou, P.C.; Fatta-Kassinos, D. Adsorption and removal of seven antibiotic compounds present in water with the use of biochar derived from the pyrolysis of organic waste feedstocks. *J. Environ. Chem. Eng.* **2021**, *9*, 105868. [CrossRef]
76. Delmond, B.; Tretsiakova-McNally, S.; Solan, B.; McDermott, R.; Audoin, A. A Sustainable Method to Reduce Vancomycin Concentrations in Water Using Timber Waste. *Water Air Soil Pollut.* **2023**, *234*, 81. [CrossRef]
77. Piaggio, A.; Mittapalli, S.; Calderón-Franco, D.; Weissbrodt, D.; van Lier, J.; de Kreuk, M.; Lindeboom, R. The fate of sulfamethoxazole and trimethoprim in a micro-aerated anaerobic membrane bioreactor and the occurrence of antibiotic resistance in the permeate. *Water Sci. Technol.* **2023**, *88*, 2344–2363. [CrossRef] [PubMed]

Disclaimer/Publisher's Note: The statements, opinions and data contained in all publications are solely those of the individual author(s) and contributor(s) and not of MDPI and/or the editor(s). MDPI and/or the editor(s) disclaim responsibility for any injury to people or property resulting from any ideas, methods, instructions or products referred to in the content.